American Physical Society - Eastern Great Lakes Section
Northern Ohio Section of the AAPT
SPS -Zone 7

Fall 2023 Meeting

Friday & Saturday, October 20-21

Cleveland State University
Cleveland, Ohio 44115

Physics at the Nanoscale

Local Co-Organizers: Dr. U. Zürcher
E-mail: u.zurcher@csuohio.edu
Dr. S. Sensale Rodriguez
E-mail: s.sensalerodriguez@csuohio.edu

Program - Outline

Friday October 20

2:00 - 2:45	Session A: Registration Fenn Tower Atrium
2:45 - 3:00	Session B: Welcome **Dr. Andrew Kersten**, Dean, College of Arts and Sciences, CSU Fenn Tower 303
3:00 - 3:45	**Session C: Dr. Fangwei Si** (Carnegie Mellon University) How bacteria organize cellular space at the microscale and the nanoscale Fenn Tower 303
3:45 - 4:00	Session CC: Coffee Break
4:00 - 4:45	**Session D: Dr. Divita Mathur**, (Case Western Reserve University) Synthetic DNA Nanostructures as Platforms for Precise Nanoparticle Organization Fenn Tower 303
4:45 - 5:00	Session DD: Coffee Break
5:00 - 6:30	**Poster Session & Social Hour** Fenn Tower Atrium 5:00 - 5:30 - Session E: Welcome from SPS - Fenn Tower 303 5:30 - 6:30 - Session F: Poster Session - Fenn Tower 303 / Atrium
6:30 - 8:00	**Session G: Banquet** (Tickets required) - Fenn Tower 303* *Free to Undergraduate Students with SPS Registration (sponsored by SPS).
8:00 - 8:45	**Session H: After Dinner Speaker** **Dr. Graham Dixon**, Ohio State University Communicating Science in the 21st Century: Challenges and Opportunities Fenn Tower 303

Saturday October 21

7:45 - 8:15	Session J: Registration and Continental Breakfast – SR Atrium
8:15 - 9:00	**Session K: Dr. Rose Cersonsky** (University of Winsconsin-Madison) Disentangling the impact of packing in colloidal and molecular self-assembly SR 151
9:00 - 9:15	Session KK: Coffee Break
9:15 - 10:45	**Sessions L1-5: Contributed Talks** - Science Bldg Contributed Talks in Parallel Sessions
10:45 - 11:00	Session LL: Coffee Break
11:00 - 11:45	**Session M: Dr. Lisa Felter** (Newry Corp) From Physics to Consulting: Life After the Lab (co-sponsored by SPS) SR 151
11:45 - 12:00	**Session N: EGLS Chair's Remarks** - SR 151 Dr. Zifeng Yang, APS EGLS Chair
12:00	**Conference Closure**

Invited Speakers

C: Dr. Fangwei Si, Department of Physics, Carnegie Mellon University
How bacteria organize cellular space at the microscale and the nanoscale
Cellular space is incredibly crowded with biomolecules yet well-organized. However, we still lack a precise understanding of how cellular spaces at the microscale and the nanoscale are spatially organized to dictate cellular scale behaviors. In this talk, I will discuss how bacteria as simple living systems organize membrane space at the microscale and the nanoscale to possibly optimize cell fitness. The organization of the cell membrane connects to its physiological state via a combination of physical, chemical, and biological processes. We are trying to disentangle this complexity by testing a fundamental hypothesis suggested by our preliminary observations: the membrane real-estate hypothesis – the cytoplasmic membrane is so packed with proteins that the cell needs to fine-tune the density, composition, and organization of the membrane proteins for optimizing cell fitness. To better test this idea, we quantify and manipulate the density, composition, and spatial organization of membrane proteins and examine their effects on physiological states such as growth, adaptation, and cell death. We will use these results to test physical models that connect membrane properties to cell physiology. The outcomes from this hypothesis-testing can help us bridge cellular organization and physiology and understand better cellular adaptation, a branch of knowledge that can be extended to studying other higher organisms.

D: Dr. Divita Mathur, Department of Chemistry, Case Western Reserve University
Synthetic DNA Nanostructures as Platforms for Precise Nanoparticle Organization
DNA nanotechnology has enabled the ability to build objects and particles at the nanoscale. With the help of a growing repository of DNA self-assembling tools and strategies, it is possible to create two- and three-dimensional structures, ranging from a few nanometers to micron-scale in size. The cumulative properties of DNA, particularly its well-studied biophysical and biochemical properties, compatibility with a host of organic and inorganic nanoparticles, and the predictable base pairing principles have led to its application as a building material in single-molecular studies, photonics, plasmonics, synthetic biology, and healthcare. Herein, I will share our work on building DNA-based platforms for the precise organization of inorganic and organic nanoparticles and biosensors. We explored the extent to which DNA platforms can control the relative positioning and orientation of these nanoparticles to augment their photophysical abilities. Results show spectral tailoring of gold nanorod architectures, efficient patterning of multiple semiconductor quantum dots, and elucidating the effect of three-dimensional dye spacing on Förster resonance energy transfer

H: Dr. Graham Dixon, School of Communication, Ohio State University
Communicating Science in the 21st Century: Challenges and Opportunities
The 21st century has brought numerous challenges to science communication. Scientists often face a skeptical public, combat mis/disinformation on social media, and must keep up with an ever-changing information environment. Further compounding these challenges is the difficulty scientists experience in translating complex information to various audiences. Solutions to these challenges are often elusive, as many so-called "common sense" communication approaches are at best ineffective, but at worst can widen the gulf between scientists and the public. This talk explores specific challenges we face and the solutions that communication research offers.

K: Dr. Rose Cersonsky, Department of Chemical and Biological Engineering, University of Wisconsin-Madison
Disentangling the impact of packing in colloidal and molecular self-assembly
Geometric packing is an oft-used causal mechanism for structure formation across many length scales – from the entropic ordering of colloidal nanoparticles to molecular co-crystallization of drug-like molecules. However, its exact role is hard-to-quantify, particularly in regimes where many competing forces can motivate nucleation, and evidently, crystallization. In this talk, I will first discuss the impact of geometric packing in systems where its effect should be most pronounced – hard, faceted nanoparticles that self-assemble based on volume exclusion alone. Using Maxwell relations, I will show that markers for "packing" behavior are absent in the regimes where self-assembly occurs, pointing to packing as a correlative, rather than causal, force in the emergence of spontaneous order. I will then shift focus to crystallization in small-molecule systems, where the role of packing is still an open question and hard to pinpoint in analyses. Using physics-based machine learning representations and hybrid supervised-unsupervised models, I show how we can identify the role of enthalpic and geometric components in stabilizing (or destabilizing) these systems. I will end with an outlook on the future of physics-informed machine learning for understanding molecular packing, including future work directions.

M: Dr. Lisa Felter, Newry Corp
From Physics to Consulting: Life After the Lab
Choosing a career path outside of academia can be intimidating - but it doesn't have to be! While there are numerous paths a Physicist could take, their training and experience solving complex problems, as well as ability to conduct deep research, makes them particularly well-suited for careers in management consulting. In this talk, we'll discuss how one Physicist transitioned out of academia to a fulfilling career in technology strategy consulting, and what she learned along the way, including: how to approach a career search, developing (the poorly-named) "soft" skills needed for a career in industry, and how she leverages her Physics training on a daily basis.

Poster Session (Fenn Tower Atrium)

F1: Phase Analysis of Charge Density Waves in Kagome Superconductors. Lily Baker (College of Wooster)
Charge density waves (CDWs) can be analyzed using Scanning Tunneling Microscope (STM) images. In this study, we demonstrate an approach to investigate CDWs by registering STM images of the same sample at different bias voltages, followed by an Inverse Fourier Transform and line cuts of the resulting images. This process allows us to create a waterfall plot, revealing the phase shift in the charge density wave. The phase shift provides crucial insights into the positioning of the Charge Density Wave gap relative to the Fermi Level. Our investigation focused on a sample of crystal CsV_3Sb_5, and we discovered that the π-phase shift occurs at an unexpected sample bias of 280 mV instead of the expected 0 mV.

F2: Constraining Curvature in Kantowski-Sachs Spacetimes with Late Time Anisotropy. Ananda Smith, Glenn d Starkman, Craig J Copi (Case Western Reserve University)
The current standard model of cosmology postulates that any large-scale spatial curvature the Universe possesses is isotropic. However, it is possible for space to possess anisotropic curvature, and such spaces remain viable candidates for describing the large-scale spacetime structure of the Universe. Here we seek to constrain the anisotropic curvature of a Kantowski-Sachs universe, a model admitting an $S2 \times E1$ spatial geometry. By solving the Einstein equations with small scale factor anisotropy, we model the expansion of this universe from last scattering onwards and examine the consequences of this anisotropic evolution on cosmological observables. We find that the anisotropic curvature of a Kantowski-Sachs universe is constrained by the quadrupole ampltiude of the cosmic microwave background.

F3: Foreground Scaling in the BICEP/Keck 2018 Likelihood. Lauren Bell (University of Cincinnati)
When studying B-mode polarization in the Cosmic Microwave Background, there is foreground emission from the Milky Way that obscures our view of the CMB. This foreground consists of dust and synchrotron radiation, where the foreground power spectra scales with angular scale. While this power-law is empirically supported when analyzing small patches of the sky, there is no theory to support this scaling. The baseline likelihood used in in the BK18 analysis uses data from multiple different telescopes, including the BICEP/Keck collaboration, WMAP, and Planck through the 2018 observation season. By using this data and separating dust and synchrotron radiation into bins based on angular scale, ι;, and changing the likelihood calculation, we make the foreground model more flexible. The new likelihood follows the initial power-law likelihood within 1σ; for both dust and synchrotron.

F4: The Angular Velocity of Dust Particles in Multi-Ring Plasmas with Agitators. William L Theisen, Anthony F Parker (Ohio Northern University)
Using a grooved electrode and a wave form generator, a plasma was created from argon gas. Due to the grooves in the electrode a confining potential well formed in the plasma. Melamine formaldehyde dust was then sprinkled onto the plasma creating a multi-ring dusty plasma. The dust particles moved in a circular path with varying angular velocities depending on the number of rings in the section they were traveling through. Among the dust particle there were agitators, which are particles that aren't laying on the same plane as the rest, meaning they rapidly jump in and out of the plane. It was observed that the angular velocity increased for sections with a smaller number of rings. The dependence of the angular velocity on the anode voltage was also investigated.

F5: Numerically Stable Resonating Hartree-Fock for Computational Photochemists. Ericka Roy Miller, Shane M Parker (Case Western Reserve University)
Nonadiabatic molecular dynamics (NAMD) simulations are powerful tools that provide atomic scale insights into photochemical processes. However, the effectiveness of these NAMD simulations is extremely dependent upon the quality of their underlying electron structure theory (EST) engine. The ideal EST method for NAMD applications will produce correct electronic state crossings and balanced descriptions of states of different character, all without breaking the computational bank. The Parker research group believes state-averaged Resonating Hartree-Fock (SA-ResHF) is a promising candidate for the next generation of NAMD simulations. The ResHF wavefunction is a linear combination of nonorthogonal Slater determinants, which affords it enough flexibility to balance the demands of electronic states of starkly different character but comes at the cost of numeric instability. In this talk, I will demonstrate the strengths of ResHF by showing how it avoids state-averaging errors that commonly plague the CASSCF method. I will then present our numerically stable reformulation of the ResHF equations, which uses singular value decomposition and the matrix adjugate to avoid numeric 'blow-ups' resulting from nearly orthogonal Slater determinants.

F6: X-ray peak profile analysis of ZnO nanoparticles obtained from sol-gel synthesis method. Khagendra P Bhandari, Peyton Burden, Manoj K Jamarkattel (Ohio Northern University)
Sol-gel synthesis of ZnO nanoparticles is the simplest method where particle size and morphology can be controlled via systematic monitoring of reaction parameters. To accomplish the synthesis method, zinc acetate dehydrate ($Zn(CH_3COO)_2$ $2H_2O$) is used as a precursor, ethanol (C_2H_5OH) and methanol (CH_3OH) as a solvents, sodium hydroxide (NaOH) and distilled water as medium. In the synthesis process, zinc acetate dehydrate and sodium hydroxide are separately dissolved in deionized water in two different vials. Sodium hydroxide solution is then added to zinc acetate dehydrate solution and mixture of ethanol and methanol are added dropwise using titration method. Zinc oxide nanoparticles so obtained are characterized by using UV/Vis/NIR spectroscopy and X-ray diffraction spectroscopy. Results obtained from UV/Vis/NIR spectroscopy measurements for both the solution and thin film are used to calculate absorbance, absorption coefficient, and bandgap of the material. Similarly, data obtained from XRD measurement are used to complete peak profile analysis. Using peak profile analysis, we approximate size of nanoparticles, their crystallinity and their crystal structure. We also calculate crystallite size of the nanoparticles, interplanar spacing, and lattice constants of the nanoparticles.

F7: Using Raman Spectroscopy to Understand Phonon Modes of Semicondcting Ternary Nitrides. Summer Carver (Case Western Reserve University)
Heterovalent ternary nitride crystals have significant promise in their potential applications due to their unique band-structure engineering capabilities. These crystals are integrable with binary nitrides, which revolutionized the solid state lighting industry and, recently, have been shown to be efficient silicon replacements within power electronics. The cation sublattice ordering and the structural periodicity of ternary nitrides greatly impacts their band gaps and lattice constants. Raman microscopic spectral analysis of crystal lattices detects phonon modes to give insight into the cation ordering. A Raman microscope is being constructed with an integrated fiber optic system between a BX60 Olympus confocal microscope, a laser, and a HoloSpec spectrometer; the inelastically scattered photons will be collected via an iDus 420 series CCD. The purpose of the microscope is to gain not only a spatial understanding of the samples by exploring the homogeneity of single crystal films on the micron scale, but also to image crystallites precipitated from and embedded within a solute metal alloy. Multiple crystals will be analyzed including synthesized $MgSnN_2$ and materials structurally related to $LiGaO_2$; various crystal recipes will be compared to explore the results of different growth procedures. These results may improve designs of future crystal growth methods to characterize and control the cation ordering within these materials.

F8: DFT Analysis of Short-Chain PFAS Absorption via Functionalized Biochar. Eric E Caldwell, Mesfin Tsige, Hansini Abeysinghe, Xingmao Ma (University of Mount Union)
Research into Per- and Polyfluoroalkyl Substances (PFAS) removal from aqueous solution has recently become a priority due to the toxicological dangers PFAS presents to humans and wildlife. This study has examined the absorbance of short-chain Perfluorobutanoic Acid (PFBA) on Biochar using a first principal computational tool known as Density Functional Theory (DFT). Biochar has shown promise as a cheap and easily scalable adsorption medium. However, Pristine Biochar has low rates of adsorption, requiring functional groups to increase its effectiveness. The computational nature of DFT means that the functionalized Biochar can be studied more quickly than in a lab setting. This helps narrow down the potential options for functional groups without needing to fully synthesize the molecules. This study examined the interaction of anionic PFBA with graphene-modeled Biochar at the atomic level. The graphene-modeled Biochar was functionalized with -NH_2, -$N(CH3)_3$, and -$CH_[2N(CH_3)_3$ groups. Five PFBA configurations were tested for each type of Biochar. Biochar functionalized with -$N(CH_3)_3$ or -$CH_2N(CH_3)_3$ was shown to be more effective at adsorbing anionic PFBA compared to Pristine and -NH_2 functionalized Biochar. Based on our results, the effectiveness of the trimethylamine group in adsorption was not hindered by the additional -CH_2. This was shown using Adsorption Energy, Minimum Interaction Length, and the Electrostatic Potential (ESP).

F9: High pressure single-molecule investigation of analyte interactions with chiral stationary phase particles. Aman Kapoor, Ricardo Monge Neria, Lydia Kisley (Case Western Reserve University)
Many molecules are synthesized as 50/50 mixtures of two mirror-image versions, termed chiral enantiomers. Separating enantiomers is essential to drug development, as each enantiomer can have varied health effects. Chiral chromatography is used to separate enantiomers but lacks a molecular-scale understanding. Previous single-molecule studies from our lab used highly inclined and laminated optical sheet (HILO) microscopy to investigate achiral analyte interactions with chiral stationary phase particles (CSPs) at pressures of 600 psi. Results showed that 2 nm analytes reach a depth of only 20% of the CSP diameter, despite CSP pores being 50 times larger than analytes. It is unknown whether the inability of analyte molecules to penetrate CSP pores is due to low operating pressures, which are below actual column pressures of 5,000 psi, or physical blockage by CSP polymer coatings. In this study, we build a high-pressure single-molecule setup to determine if pressure changes analyte penetration into CSPs. We pack CSPs and analyte into optically-transparent capillary tubes compatible with fluorescence microscopy and couple the capillary tube to a pressure generator that can achieve 5,000 psi. We image the packed capillary tubes with HILO microscopy and analyze single-molecule locations with super-resolution algorithms. We hypothesize that high pressures will not cause analyte molecules to penetrate the porous particles and that the lack of analyte penetration can be attributed to the polymer coating.

F10: Study of micromixing systems employing extensional flows. James S Taton, Chandrasekhar Kothapalli, Petru S Fodor (Cleveland State University)
Using computational fluid dynamics, the effect of implementing constrictions, defined by inverse functions, on the mixing performance of microfluidic devices operated in the laminar flow regime is investigated. The proposed designs combine uniform stretching flows generated by the hyperbolic constrictions with sheer flows resulting from the centripetal forces experienced by the fluids as they are directed along serpentine channels. Data showed that the mixing index is maximized for narrow and long constrictions. However, the required pressure differential for this global maximum in the mixing performance is also increased. Using in addition to the absolute mixing index measure, a cost of mixing measure as well, allows for a better optimization of the designs.

F11: Growth of gallium oxide nanowires on a gold coated silicon dioxide wafer. Samuel S Hertzer, John E Treusch (Grove City College)
Gallium oxide is a likely wide bandgap semiconductor with many potential applications. To understand the characteristics of this material, we use the vapor-liquid-solid (VLS) growth technique to synthesize gallium oxide nanowires. Such growth is dependent on numerous initial conditions, such as thickness of the metallic catalyst coating (gold) on the silicon wafer substrate. Precise control of these initial conditions has proven to be very difficult. We believe gallium oxide nanowire growth should be directly correlated with the thickness of gold coating on the substrate but our results to date have been inconclusive. More work is required to determine the relationship between gallium oxide nanowire yield and gold coating thickness.

F12: Unfolding the rheology and microstructure of bidisperse soft jammed suspensions under shear flow. Rakan M Alrashdan, Fardin Khabaz (University of Akron)
Soft particle glasses (SPGs) are yield stress fluids that consist of deformable particles that are jammed at volume fractions above the random close packing of equivalent hard sphere suspensions. SPGs flow when they are under stresses that are larger than their dynamic yield stress. These features allow them to be used in various applications such as cosmetic products, coatings, and pastes. However, these suspensions show a glassy structure at low shear rates and transform into a layered phase at high shear rates when the particle size distribution is narrow. In this study, a series of bidisperse suspensions are considered, and the relationship between the microstructure and macroscopic rheology is probed using particle dynamics simulations. Results show that at high shear rates, bidisperse suspensions exhibit a glassy structure when the number ratio of big to small particles is between 0.1 and 0.2, and the ratio of big to small radii is between 1.60 and 1.70. In this regard, a comprehensive phase diagram based on the applied shear rate, particle size ratio, and the ratio of the radii in shear flow is provided. These results provide an alternative method to control the phase behavior of the soft suspensions compared to the conventional understanding which requires a broad particle size distribution.

F13: Dynamics and Mechanical Properties of Hybrid Vitrimer Networks. Harsh Pandya, Fardin Khabaz (University of Akron)
Vitrimers are associative crosslinked polymer networks that exhibit properties of self-healing, network integrity, solvent resistance, and reprocessability. The presence of dynamic covalent bonds allows these networks to undergo topology alterations by applying stimuli such as heat or deformation. One of the proposed methodologies to improve the mechanical properties of vitrimers and mitigate undesirable creep at low temperatures is to create hybrid networks consisting of both dynamic and permanent covalent linkages. The primary objective is to determine a critical concentration of the dynamic bonds to suppress low-temperature creep while retaining the self-healing and reprocessability of vitrimer networks. We use hybrid Molecular Dynamics - Monte Carlo simulations to study the dynamics of glassy vitrimer networks with varying concentrations of reactive sites by subjecting them to triaxial stretching experiments and comparing their behavior to permanently crosslinked networks. Results show that the networks undergo crazing through the bulk, followed by ultimate failure. The vitrimer networks show a higher strain at fracture than the permanently crosslinked network, and this strain is a direct function of the number of available reactive sites in the network. Furthermore, Vitrimer networks under triaxial stress successfully relax stress by means of bond exchange reaction even in the glassy regime.

F14: Microscopic Morphology and Dynamics of Bridged and Pendant Ionomers. Nazanin Sadeghi, Fardin Khabaz (University of Akron)
We performed molecular dynamics (MD) simulations using a coarse-grained model of ionomers with distinct chain architectures, in which both types of ions are incorporated in the polymer chain (bridged structure) and compared their dynamics and structures with the conventional pendant ones where counterions are freely added to the system. Our results showed that the glass transition temperatures of both structures are comparable and slightly higher than the corresponding control system. Mesoscale ordering existed within large, percolated aggregates in the bridged structure and between distinct aggregates seen in the pendant structure. Also, long-range order was seen in the percolated ionic network of the bridged structure. Dynamical heterogeneities were seen even at temperatures above Tg in both structures, which persist at higher temperatures for the bridged ionomers, indicating the preservation of the ionic network at higher temperatures in the bridged ionomer. Analysis of the dynamics of the physical bonds and the intermediate scattering function showed a linear correlation between the lifetime of the ionic bonds and the dynamical relaxation time over a wide temperature range. A comparison of these time scales showed that in the bridged ionomers, ions have collective dynamics, unlike the pendant structure in which ion-pair dissociation occurs before escaping the local environment. Furthermore, our results show that the ISF data in both structures can be collapsed onto a master curve that confirms the applicability of the time-temperature superposition principle in these structures. Overall, this study shows that incorporating ions in the backbone provides an alternative route to control the morphology and dynamics of the ionomers.

F15: Cross-Correlation with Fluorescence Correlation Spectroscopy Super-Resolution Optical Fluctuation: Improved Imaging at the Nanoscale. Benjamin G Wellnitz, Jeanpun Antarasen, Stephanie Kramer, Lydia Kisley (Case Western Reserve University)
Research into the extracellular matrix (EMC), a porous network structured with macromolecules and minerals which surround the cells, allows for future applications such as improved drug delivery systems. The diffraction limit of light makes structures on the scale of the wavelength of light difficult to distinguish due to the convolution of a point spread function (PSF) in widefield microscopy. Here we are using an imaging technique ¡em¿via¡/em¿ microscopy called fluorescence correlation spectroscopy super-resolution optical fluctuation (fcsSOFI) to image EMC like hydrogel environments. fcsSOFI combines two previous methods (FCS and SOFI) to image both the diffusion dynamics and structure of ECM like materials. FCS utilizes auto-correlation curves to calculate diffusion coefficients. SOFI utilizes independent fluorophores and auto-correlation to gain a higher resolution with a squared point spread function. Here we are implementing cross-correlation SOFI to allow for a higher sampling rate via the creation of interpolated pixels between the original pixels (thus allowing for a four-fold increase in pixels). Since a SOFI image covers the same physical distance whether using auto or cross-correlation, second order cross-correlation doubles our sampling frequency. We can now identify structural features twice as small without any aliasing in our fcsSOFI images, allowing us to gather even more structural information about our EMC like environments at the nanoscale.

F16: Iterative reconstruction of two-dimensional sinograms with TomoPy for magnetic particle imaging. Chris Bastajian (Oakland University)
Tomographic projection imaging technique is well recognized for its reliance on sinograms. Sinograms are the result of imaging scans in the field of medical imaging: CT, PET, etc. One of the more recent techniques that uses projection imaging is Magnetic Particle Imaging (MPI). In MPI, a subject with an injected nanoparticle tracer can be imaged using a magnetic field free line (FFL) at various angles like an X-ray beam in CT. Such imaging produces 2D sinograms that are generally reconstructed through inverse radon transformation. While this technique, coupled with filtered back-projection and deconvolution, approximates the subject's original characteristics effectively, it has some limitations that need to be improved in MPI: imaging artifacts and low spatial resolution. To address this objective in our MPI scanner, we opted to employ a hybrid iterative tomographic reconstruction in Python using TomoPy's libraries, standardly used for reconstructing 3D sinograms, to reconstruct a wide range of 2D data with a variety of iterative methods. Notably, this study introduces an effective method to manipulate 2D matrices and reconstruct their corresponding sinograms providing better image quality in MPI.

F17: Optical Trap Generation Using Spatial Light Modulator (SLM) for Investigating Primary Ciliary Mechanics. Pinak Deshpande, Andrew H Resnick (Cleveland State University)
The primary objective of our laboratory is to investigate the mechanical properties of cilia within biological cells, which serve as crucial mechanical sensing transducers. To examine the mechanical responses of primary cilia to imposed mechanical forces, we have constructed an experimental setup consisting of a laser tweezer system that uses a spatial light modulator (SLM) to steer the trap. The SLM serves as a versatile optical modulator, enabling the generation of multiple moving independent optical traps, each capable of applying a controlled force, which we will use for mechanical manipulations of individual cilia. Our current effort focuses on programming the SLM to create two independent optical traps: one remains a static position while the other translates, exhibiting user-controlled sinusoidal oscillations within the trapping plane. These oscillations are parameterized by amplitude and frequency provided by the user. We will present a user-friendly interface (UI) that integrates the SLM control software with MATLAB. We have performed basic calibration measurements as well. This system represents a sophisticated opto-mechatronic platform, merging precision optics, biological microscopy, and computational control to advance our understanding of ciliary mechanics.

F18: Developing and Investigating the Response of an SRAM Dosimeter for Use in Radiation Effects Facilities. Grace M Metz, Henry L Clark, Ethan Henderson, Cody E Parker, Ryan Rinderknecht (Case Western Reserve University)
The Texas A&M University Cyclotron Institute's Radiation Effects Facility (REF) provides researchers with heavy ion beams to test their electronics for use in terrestrial and aerospace applications. Reliable dosimetry is currently provided at the REF through the use of scintillator detectors, but a more mobile option would be beneficial to users at the REF and other facilities to verify their beams. A mobile dosimeter system using the response of an SRAM chip demonstrates total error cross section and multiplicity dependencies on linear energy transfer (LET), allowing for two distinct ways of characterizing the incident beam. In this project, improvements to the original dosimeter printed circuit board (PCB) were implemented, including a new mounting solution for quicker set-up, a reduction of electronic signal noise, and the ability to easily switch out the SRAM under test. The response of the redesigned dosimeter was tested using undegraded 40 MeV/u 78Kr ions, which were also degraded to lower energies to obtain a series of LETs, to confirm its LET-dependent response. Part-to-part variation was also investigated by exposing multiple SRAM chips to the beam.

F19: Nonperturbative prediction of Nonlinear optical properties using Action Lagrangian applied to 1D Harmonic oscillator model. Abhijith Kumar, Shane M Parker (Case Western Reserve University).
Nonlinear optical properties are the optical properties of the materials which depend on the intensity of the illuminated light. These properties occur when the polarization induced in the material is not directly proportional to the intensity of light. Nonlinear optical (NLO) properties are intensely studied for their rich fundamental physics and chemistry and because they are central to technologies like spectroscopy, bioimaging, and optical limiting. The primary theoretical approach to predicting NLO properties is through response theory. However, response theory is inherently perturbative and thus may converge slowly for moderate field strengths. Here, we introduce the Action Lagrangian Eigenvalue Problem (ALEP), which will allow us to calculate nonperturbative NLO properties directly at a moderate electric field strength. As an example, we apply the ALEP method to a one-dimensional harmonic oscillator interacting with an electric field of moderate field strength. We will show that for weak and moderate field strengths, NLO properties obtained using i) response theory, ii) quantum dynamics, and iii) the ALEP are all equivalent, thus showing that ALEP is a promising strategy.

F20: Comparing Machine Learning Methods on Synthetic Laser Accelerated Proton Data. Aditya Shah, Thomas Y Zhang, Ronak Desai, Chris Orban, Joseph R Smith (Marietta College)
The rapid advancements in laser systems have enabled high-speed data acquisition with kHz repetition rates. However, due to the complex nature of laser-matter interactions and the limitations of analytical and computational methods, accurately characterizing their features remains challenging and costly. In this research, we harness the potential of machine learning to emulate laser interactions using synthetic datasets. By comparing the performance of neural networks, decision trees, and random forests, we identify effective and efficient approaches for analyzing real-world laser datasets generated by emerging laser systems.

F21: Performing Small Angle X-ray Scattering (SAXS) on Polystyrene Probes and Polysaccharide Microgels. Patrick Herron, Collin P Douglas, Kiril A Streletzky (Cleveland State University)
Small angle x-ray scattering (SAXS) is a scattering technique that can be used to determine the average size, shape, and internal structure of nanoparticles in solution. Visible light scattering can also be used to determine size and shape distributions, but SAXS provides a wider q-range and ability to probe internal structures. The higher q-range also allows examination of smaller particles and portions of large particles. Unlike visible light scattering, SAXS yields information on the internal structure of particles as X-rays penetrate many non-transparent materials and have enough resolution to probe small structural elements. This project is focused on SAXS measurements of polystyrene spherical standards of various sizes (24-450 nm in diameter) with eventual goal of applying it to similarly sized polysaccharide microgels. Here we present the results obtained from SAXS measurements at Kent State University using the Xenocs Xeuss 3.0 system using a procedure developed by us. Our SAXS results on polystyrene hard spheres generally agree their specs. Our initial microgel results are much more tentative. Moving forward, we plan to expand our microgel runs applying the vast experience of SAXS on polystyrene probes with hopes to gain some information on the internal structure of the microgels.

F22: Solvent Effects on the Interaction of Charged Nanoparticles. Joseph Ball, Sebastian Sensale (Cleveland State University)
Self-assembly is ubiquitous in nature, allowing for the bottom-up construction of ordered structures via non-covalent interactions. These mechanisms have found multiple applications in chemistry and materials sciences, providing low-cost, highly reproducible, highly tunable strategies for the construction of multidimensional structures with very high yield. The goal of this project is to computationally demonstrate a novel technique for tuning nanoparticle aggregation by controlling nanoparticle-solvent interactions at the molecular-level.

F23: Effective Conductivity in Thin Copper Film Growth with Au Sputtered Contacts. Dennis E Kuhl, Kaitlyn Stewart, Aaron Rohr (Marietta College)
A Si (100) wafer cleaned in acetone and methanol was placed into a sputter coater where gold contacts were deposited. A 72 nm Cu film was then grown on the Si in a thermal evaporator using 99.9999% Cu wire. The resistivity of the film was measured during growth. The Fuchs-Sondheimer Scattering Model was used to analyze the effective conductivity as a function of thickness. The model only fits our data over a very narrow range of thickness. Fit parameters were $l = 13.3\,\mathrm{nm}$, $\sigma_0 = 21.4\,\mu\Omega\mathrm{m}^{-1}$, and $t_0 = 32.4\,\mathrm{nm}$. More experiments are needed to study how the gold sputtered contacts affect the electrical measurements.

F24: Time and Energy Resolution of LYSO and SiPM Detectors for Testing CP Conservation. Leonardo Juarez, Elizabeth A George, Paul A Voytas (Wittenberg University)
We will be testing charge conjugation parity (CP) conservation in positronium (Ps) decay. To do this we will use silicon photomultipliers (SiPM) and Lu1.9Y0.1SiO5 (LYSO) scintillation crystals to detect Ps annihilation radiation. I developed a procedure to test the timing and energy resolutions of our detectors. I created a testing setup that holds our detectors and a source of radiation. I developed a method for offline constant fraction discrimination (CFD) from a digitized SiPM signal. From this we obtain a coincidence pulse time difference histogram. We determine time and energy resolution by fitting gaussians to peaks in the time and energy histograms. Details of the CFD method and results will be presented.

F25: The impact of etching β-Ga_2O_3 substrates to reduce interfacial silicon. Mark Gordon, Said Elhamri, Kurt Eyink, Brenton Noesges, Thaddeus Asel (University of Dayton)
One of the most promising materials in the past decade is $\beta{-}Ga_2O_3$. $\beta - Ga_2O_3$ is an ultra-wide band gap semiconductor material that is of great interest due to its large breakdown field and the availability of the native substrate. One problem that faces $\beta - Ga_2O_3$ is the presence of interfacial silicon that creates parasitic conduction channel, limiting the potential of devices made of $\beta - Ga_2O_3$. This work investigates methods to reduce interfacial silicon on $\beta - Ga_2O_3$ substrates. These films are grown via Molecular Beam Epitaxy (MBE), we use Secondary Ion Mass Spectrometry (SIMS) to observe the changes in interfacial chemical composition, and we utilized Atomic Force Microscopy (AFM) to observe the effect the substrate preparation will have on the surface of the substrates.

F26: A New Disease Detect and Capture Device: CAPGLO. Patrick M Deluca, Robert J Deissler, Charlotte L Bimson, Robert W Brown (Case Western Reserve University)
Many serious diseases including cancer are treatable and even curable if they are discovered and treated at an early stage. The principal objective of this work is to create an early detection - and capture - system that is accurate, quick, and portable, as well as one that can be manufactured and utilized at a low cost. Capturing enables subsequent laboratory study to determine the strain or variant of the specimen. The science and engineering of 'magnetofluoresis' - our variation on the general study of magnetophoresis - that leads to the development of the device is also investigated. We describe tests carried out with representative, sufficiently sophisticated cells. We coat insect cells as fluorescent functionalized groups and image them using a small digital microscope. With the ability to locate the individual cells and attach micron-sized magnetic particles to them, even a single cell can be guided into a tiny pocket of a sample cuvette with a gradient magnetic field. A digital microscope combined with a filter for fluorescence reading can be used to prove the cell was indeed captured. The device, with a 3D-printed cuvette, fluorescent dye, and MPs coated with a binding agent, was used to test our ability to detect the target cells. The gradient field draws the resultant MP-cell clusters into the collection region of the sample holder. The 'glowing' signal seen in the collection region indicated the presence of captured cells. The cells were then imaged with an inexpensive microscope and counted with software. We thus have a working prototype: a new low-cost fluorescent digital camera/filter/laser detection system for both capturing and counting the recovered cells. Current work is directed toward comparing the sensitivity levels with the different cancer concentrations in the human body. The total prototype cost including the cuvette is $\sim$ \$300 for the system, which strongly suggests a (much) lower unit cost for large-scale manufacturing.

F27: Light and Color - Bringing Physics to Students Beyond STEM. James Dakin.
Light and color can bring physics to students well outside STEM. The honors seminar that I am teaching at Appalachian State University in Boone, NC, is doing this. My 150-minute class each week starts with a 30-minute lecture progressing from the big bang to the present over the semester, featuring not just equation-free science, but familiar applications. (1) Each week a different Guest Expert has 30 minutes to tell about a passion. These passions range from the color of birds to early religions, photography, and the invention of the light bulb. The real key to the course is asking each student to select a topic of personal interest, learn about it from scholarly sources, and make oral presentations to classmates as knowledge builds. I argue that scholarly research and oral presentation are valuable skills no matter what career a student pursues. Topics chosen range from optical illusions (a math major), Christiaan Huygens (a history major), Seasonal Affective Disorder (a psychology major), psychology of color (a marketing major), and the greenhouse effect (a sustainable technologies major). The term paper requirement at the end is an annotated bibliography on the topic.1 Dakin JT. Wrestling with Light - History, Science and Applications. New York, NY: AIP Publishing; 2021.

F28: Harnessing Multi-Fidelity Design, Analysis, and Optimization Techniques to Advance Fusion Reactor Design. Greta I Hibbard, Jacob A Schwartz (Ohio University)
The design of fusion reactors necessitates a comprehensive assessment of interacting components to ensure engineering and economic feasibility. Complex systems, like fusion power plants, are often preliminarily modeled using low-fidelity 'systems codes' for efficient design space exploration. This paper investigates applying aerospace-derived multi-fidelity techniques to incorporate higher-fidelity models while expediting system convergence and optimizing plant design. Multi-fidelity analysis utilizes high-fidelity models to locally calibrate low-fidelity models. We automate the integration of high-fidelity and low-fidelity models using Gaussian process regression, a Bayesian machine learning method. Low-fidelity power law models are 'trained' using high-fidelity models. Gaussian Process Regression is used to estimate the error of the low-fidelity model as design points vary from the initial training data set. If the error is large for a given design point, the point is added to the training set for the high-fidelity model, and the system is re-evaluated. It was found that Gaussian Process Regression as used in this algorithm offers greater advantages at higher fractional uncertainties (148 high-fidelity model evaluations saved after 300 total points requested when $u = 0.3$) while being less advantageous at lower fractional uncertainties (5 high-fidelity model evaluations saved after 300 total points requested when $u = 0.1$). It was additionally observed that constricting input parameters to smaller value ranges resulted in more saved high-fidelity model evaluations compared to previous tests (155 high-fidelity model evaluations saved after 300 total points requested when $u = 0.3$).

F29: Approaches to Analysis of Depolarized Dynamic Light Scattering Data on Solutions of Elongated Particles.. Geofrey M Nyabere, Phil Dee, Kiril A Streletzky (Cleveland State University)
As a researcher studying nanoparticles in the sub-micron range in a Depolarized Dynamic Light Scattering (DDLS) experiment, accurately determining their size and shape is crucial. However, an analysis of collected intensity correlation data requires considering appropriate assumptions and various geometrical models, which can be challenging. Our project is aimed to provide researchers with efficient tools to analyze DDLS using two approaches and appropriate assumptions. Overall, we focused on three geometrical models: de la Torre's straight cylinder, Perrin's prolate ellipsoid, and Martchenko's spherocylinder. In the first approach, we used a multiangle DDLS experiment to obtain translational and rotational diffusion coefficients from analysis of measured intensity correlation function at various angles and then solved for geometrical anisotropy of the particles using the geometrical models. In the second approach, we followed Glidden and Muschol to analyze single scattering angle correlation functions and then used the deduced decay rates to solve for particle dimensions using the same geometrical models. To make the complicated analysis more efficient, we created a Matlab graphical user interface program that utilizes both approaches and the three geometrical models to obtain the dimensions of elongated particles. The Matlab program was tested on our previously obtained DDLS data on aqueous solutions of elongated particles prepared at different concentrations. The deduced particle dimensions at extrapolated zero concentration are an important test of the models as they all rely on the assumption of infinite dilution.

F30: Engineering Phononic Devices to Increase Functional Temperature of Quantum Technologies. Riley J Barrett, Said Elhamri, Chandriker K Dass, Piyush Shah, Debanik Das, Robert G Bedford (University of Dayton)
The study of phononics is focused on engineering lattice vibrations and heat transport in solid-state materials through nanofabrication and material strain. The quantum states that are fundamental to quantum technologies face the issue of decoherence due to phononic interactions which exist at finite temperatures causing quantum devices to typically need to be cooled down to low temperatures ($< 1\,\mathrm{K}$) for operation. In order to make quantum technologies available at higher temperatures, it is required to develop a better understanding and ability to engineer the phononic environment. With this in mind, we are attempting to create devices with a phononic bandgap at low frequencies (10s of MHz) in order to begin showing how phononic crystals can suppress or amplify signals as a function of frequency. By changing the shape, size, and relative distance of the holes on our phononic crystal membrane, we are able to manipulate the phononic bandgaps of these devices. As we move further into this project, we want to use these types of devices to create phononic cavities and shields, which are crucial to optomechanical systems.

F31: Analyzing T640 Data for Real-Time Cleanroom Air Quality Management. Nicholas S Haught, Juan C Ramirez-Dorronsoro (Marietta College)
Cleanrooms are engineered spaces, which maintain a very low concentration of airborne particulates. They play a critical role in the semiconductor and pharmaceutical industries to guarantee high quality products. This research introduces the Teledyne T640, a real-time, continuous particulate matter (PM) mass monitor, to explore cleanroom standards and air quality. The T640 monitor provides PM mass concentration after converting particle counting (counts per cubic meter) into mass concentration. This instrument is used currently by most of the U.S. state environmental agencies to monitor PM2.5. This research aims to create an application that takes de original particle counting capabilities of the instrument and use it to classify a research room in accordance with ISO cleanroom standards. This knowledge of particle counting using the T640 will improve student learning experiences to classify cleanrooms. The primary data collection involves particle count analysis across 256 size channels. A desktop application was created to communicate to the T640 and extract particle data continuously for over 200 minutes. The gathered data gave a total of 1,502,012 particulates per cubic meter of air in the research room, with 99% below PM2.5. Through analyzing the data, it was determined that the research room was classified as a class 7 cleanroom. Cleanrooms in the semiconductor industry usually operate at class 5 and below, which has less concentration of particles in the air. Future experiments could compare the T640's data to that of a dedicated cleanroom particle counter. This project serves as a steppingstone for optimizing cleanroom classification methods using versatile air monitoring devices like the T640.

F32: High-dimensional quantum key distribution implemented with biphotons. Mhlambululi Mafu (Case Western Reserve University)
We present a high-dimensional measurement device-independent (MDI) quantum key distribution (QKD) protocol employing biphotons to encode information. We exploit the biphotons as qutrits to improve the tolerance to error rate. Qutrits have a larger quantum system; hence they carry more bits of classical information and have improved robustness against eavesdropping compared to qubits. Notably, our proposed protocol is independent of measurement devices, thus eliminating the possibility of side-channel attacks. Also, we employ the finite key analysis approach to study the performance of our proposed protocol under realistic conditions where finite resources are used. Furthermore, we simulated the secret key rate for the proposed protocol in terms of the transmission distance for different fixed amounts of signals. The results prove that this protocol achieves a considerable secret key rate for a moderate transmission distance of 90 km by using 1016 signals. Moreover, the expected secret key rate was simulated to examine our protocol's performance at various intrinsic error rate values, Q = (0.3%, 0.6%, 1%) caused by misalignment and instability due to the optical system. These results show that reasonable key rates are achieved with a minimum data size of about 1014 signals which are realizable with the current technology. Thus, implementing MDI-QKD using finite resources while allowing intrinsic errors due to the optical system makes a giant step forward toward realizing practical QKD implementations.

F33: DNA Origami Motifs for Fast Localized Communication. Mathew Ogieva, Sebastian Sensale (Cleveland State University)
Over the past decades, dynamic DNA origami structures have emerged as promising candidates for nanoscale signal and cargo transport. Despite relatively fast diffusion rates, these structures face limitations in communication speed due to the reaction-limited nature of strand exchange mechanisms used for signal and cargo transfer. In this study, we explore how spatial confinement can expedite communication among DNA walkers and compare two potential mechanisms: one that constrains molecular motion to pseudo-rotational dynamics, and another that confines it to pseudo-linear dynamics. Using stochastic theories, we suggest that a combination of both mechanisms yields the highest velocity enhancement. This study offers novel insights into leveraging structural motifs to optimize signal propagation rates, with implications for sensing and computing applications in reaction-diffusion systems.

F34: Temperature to polarization leakage using BICEP3. Eli Meisel (University of Cincinnati)
Temperature to polarization leakage is one way for systematic noise to be interpreted as data. Using shapelets, we parameterize data from BICEP3. Detectors come in pairs and the pair difference shows the temperature to polarization leakage. We simulated temperature to polarization leakage from the differential shapelet coefficients at different expansion orders. Statistics were taken to create potential CMB S4 beams for further analysis. In the future, this analytical tool can be used to further explore current and future data when looking for temperature to polarization leakage.

F35: How Improbable is Our Universe? The Uncorrelated Anomalies of the Cosmic Microwave Background. Joann E Jones, Glenn d Starkman, Craig J Copi (Case Western Reserve University)
The cosmic microwave background (CMB) can be described as a snapshot of the early Universe. It provides us with essential information on the origin and evolution of the Universe. Using the CMB, we are able to place constraints on the current standard model of cosmology, λCDM. Conventionally, λCDM treats the Universe as statistically homogeneous and isotropic, i.e. the same in every location and in every direction. However, there are several unexpected features of the large scale fluctuations in the CMB that are inconsistent with statistical isotropy. These are referred to as the large-scale anomalies. Each of these anomalies has a small chance of occurring (0.01 - 1%), but they are often individually excused as statistical flukes. In this project, we seek to answer the question of whether or not these anomalies are correlated. In particular, we are interested in the lack of large-angle correlation, the odd-parity preference, the quadrupole-octupole alignment, and the hemispherical asymmetry anomalies. We find that the anomalies we have considered are uncorrelated in the tails of their distributions, meaning that their joint probability is significantly lower. We place an upper limit of 0.003% on λCDM reproducing our CMB. This provides strong evidence against the existence of statistical isotropy in our Universe.

F36: Intermediate-range order in Organic Glasses. Spoogmay Khan, Gang Chen (Ohio University)
Intermediate-range order (IRO) is a unique phenomenon of glasses. An important structural signature of the IRO is the so-called first sharp diffraction peak (FSDP) that appears at a low scattering vector position (¡ 2Å-1) of the X-ray or neutron scattering patterns of the glasses. Although FSDP has been observed in many different glass systems, its structural origin remains elusive and seems to be specific to individual glass systems. The IRO has been studied extensively in inorganic glasses but very few efforts have been dedicated to organic glasses. In this paper, we select a simple organic glass system(i.e.,polystyrene) as a model system to understand the effect of molecular weight and temperature on the FSDP. We also study the effect of radiation on the FSDP using neutron radiation generated from the 4.5-MV tandem accelerator at Ohio University. The effect of radiation dose on the FSDP will also be discussed.

F37: Analysis of the ADCs for Stellar Intensity Interferometry. John Scott (The Ohio State University)
In this poster, I will analyze the analog to digital converter (ADC) signal received from each of the four telescopes in VERITAS (the Very Energetic Radiation Imaging Telescope Array system) that we use to provide measurements of the angular diameter of stars. Located in Arizona, the array is primarily used for ultra-high energy gamma ray astronomy. During the full moon when gamma ray astronomy is not possible, the stellar intensity interferometry (SII) group makes use of these telescopes by observing light at a wavelength of 416 nm. The four telescopes provide six pairs with baselines that range from about 35-170m and our observing runs range from 30 minutes to 2 hours. Each of the four telescopes provides its own ADC, which is a measurement of light intensity obtained from photomultiplier tubes (PMTs) on the telescope. The ADC from one telescope is then correlated over the entire length of the run with the ADC from another telescope in the array. The correlation function produced by this process shows a small signal with magnitude on the order of 10e-6 that is known as the 'HBT peak', named after Hanbury Brown and Twiss. The HBT peak is an observed increase in probability of measuring photons from the same source at the same time which, based on this peak and the distance between the telescopes, can be used to give a measurement of the angular diameter of the star. While the individual ADCs do not tell us much about the HBT peak, there is still plenty to learn from an ADC signal before it is correlated with another telescope. By analyzing how the ADCs change as time progresses in the run, we can find characteristics in the signal and detectors and make insights on how they may be affecting our measurements of the stars. One such characteristic is afterpulsing, a type of feedback where the received signal overloads the detector and spreads the signal out over a longer period of time. This can cause uncertainty in the timing of our signal, which is key when correlating it with another ADC to find the HBT peak.

F38: Max-Cut Problem: Effect of depth on the Quantum Approximate Optimization Algorithm. Je-Yu Chou, Mhlambululi Mafu (Case Western Reserve University)
Compared to classical technologies, quantum technologies demonstrate tremendous potential for providing computational advantages in various fields. We investigate the effect of the depth of the circuit on the performance of the Quantum Approximate Optimization Algorithm (QAOA). The QAOA algorithm, a hybrid quantum-classical variational algorithm, is intended to provide a quantum advantage in finding approximate solutions to combinatorial optimization problems. It has demonstrated capability in computing graph partitions with maximum separations between edges, also known as maximum cuts (max-cut). The max-cut problem belongs to the class of nondeterministic polynomial (NP) combinatorial optimization problems. To solve this problem, we define the cost function and translate it to the Hamiltonian of the system by substituting the bitstrings as Pauli Operators. In order to simulate the experiment, an ideal simulator and a noisy simulator were used, which modeled thermal relaxation errors, and the results were compared with a table of the values for the cuts which had been performed in a conventional manner. Our results demonstrate that increasing depth does not increase the average cut value in either simulator. Furthermore, the noisy simulator generally produces a lower cut value than the noiseless simulator.

F39: Analyzing Avalanche Patterns on a Conical Bead Pile. Aeralyn Flynn, Susan Y Lehman (College of Wooster)
A conical bead pile is used as a model critical system to investigate granular avalanches and criticality. The pile is roughly 20,000 beads, each 3 mm in diameter, and the system is driven by dropping one bead at a time onto the apex of the pile. This research focused on the size and frequency of avalanches in the system. We studied how closely our avalanche system follows the geophysical earthquake model Omori's law, which states that the frequency of smaller events follow a power law distribution before and after the earthquake mainshock. Three different avalanche analysis routines were created to study the frequency of avalanches over any given run, and how the frequency varies over the course of a run. The first algorithm picks out the largest avalanches in the system within a specific interval and sets these as the 'main avalanches' in the run. The second analyzes how many avalanches occur between two main avalanches and calculates the probability of an avalanche occurring in general during a given interval. Finally we find the avalanche occurrence rate in an interval immediately preceding and following each main avalanche. The optimal threshold size for a main avalanche and the length of the relevant pre-/post-avalanche time interval are being determined. We present preliminary results on the size of main avalanches in relation to how many avalanches occurred overall and in relation to the frequency of avalanches in the interval preceding and following the main avalanches.

F40: Role of flow-induced dynamical heterogeneities in macroscopic rheology of soft particle glasses. Hrishikesh M Pable, Michel Cloitre, Fardin Khabaz (University of Akron)
Soft particle glasses (SPG), which are jammed beyond the random close-packing fraction of equivalent hard spheres, show rich rheology under shear flow. The softness of particles allows them to compress to volume fractions larger than the random close-packing and form flat facets at the contact between particles. In this regime, the thermal energy contribution becomes minor, and the contact forces are the dominant source of dynamics and govern the morphology and macroscopic rheology. These fluids demonstrate yield stress behavior and flow according to the Herschel-Bulkley (HB) relationship. In our study, we have used our particle dynamics numerical method to establish a relation between the various factors that affect the microscopic dynamics and rheology of these flow-induced SPG systems; some of these factors being the volume fraction of the particles, nature of the solvent and the strength of the flow. The analysis of the shear flow curves and the trajectories of particles have shown strong evidence of dynamical heterogeneities in the system. The length scale of the domains of these heterogeneous motions is linked to the stress-strain behavior at low and high shear rates. Furthermore, the study of the non-affine square displacement shows the presence of avalanches in the dynamics of the system. These results establish a direct relationship between the microscopic dynamics of SPGs and their macroscopic properties that can be utilized in designing yield stress fluids.

F41: Ex-Situ Ellipsometry of Doped Gallium Oxide Thin Films Abstract. Eric Johnson, Narmin Ibrahimli, Ilhom Saidjaforzoda, Necmi Biyikili (College of Wooster)
Atomic Layer Deposition (ALD) is a self-limiting, precise chemical vapor deposition technique used to build semiconductors. This process involves depositing two or more precursors onto a Silicon or Saphire wafer preceding surface layer reactions, creating a thin monolayer film from the reactants. These films are used in many modern technologies, from hydrogen fuel cells to photovoltaic solar cells to gas sensing technology. This research used ex-situ ellipsometry to characterize doped and undoped gallium (III) oxide's (Ga2O3) thickness and refractive index. Films were randomly chosen for ex-situ annealing at 650℃. From this ex-situ ellipsometry, we could see that the recipe affected the thickness, with the Silicon doped being smaller, around 46.607 nm, and the Tin doped being larger, around 65.207 nm. The undoped or lightly doped films were between 54.408 nm and 56.695 nm. The change in recipe had no change in the refractive index. Annealing of the films changed both the refractive index and the thickness of the film, with annealed films having a smaller refractive index and a larger average thickness. Our results allow us to better characterize gallium (III) oxide films, doped and undoped, printed from Atomic Layer Deposition, and apply them to modern technologies.

F42: Spin diffusion and dynamical susceptibility of Kitaev spin liquid. Salim Karimov (Ohio State University)
Quantum spin liquids (QSLs) are exotic phases of matter that exhibit disordered spins even at absolute zero temperature, yet possess stable topological order. Among various QSL models, the Kitaev model on a two-dimensional honeycomb lattice has become a paradigmatic system due to its intriguing properties, including topologically non-trivial gapless ground states and fractionalized excitations. The potential application of these fractionalized excitations in quantum computing has generated considerable interest in the field. In this study, we elucidate the absence of spin diffusion in Kitaev QSLs at any temperature by leveraging the integrability of the Hamiltonian. Our analysis demonstrates that local magnetic perturbations induce no spin diffusion, as confirmed by numerical results. We show that this absence of diffusion is not solely due to short correlation lengths but also arises from anisotropy in correlations, both originating from conserved Z2 flux. Furthermore, we investigate the dynamic magnetic susceptibility of different Kitaev phases and its dependence on temperature. This analysis complements recent experiments and may serve as an observable probe for the elusive topological quantum phase transition in Kitaev models. Our findings contribute to a deeper understanding of quantum spin liquids and their potential applications in quantum computing, emphasizing the unique transport properties of these exotic quantum states.

F43: Performance Study on High Level Trigger for Vector Boson Fusion Process in CMS Run 3 Data at $\sqrt{s} = 13.6$ TeV. Raymond Kil (Boston University)
The Compact Muon Solenoid (CMS) comprises a two-level trigger system that selects and stores potentially interesting proton-proton collision events in light of reducing a large fraction of well-known background and efficiently managing the data produced at the Large Hadron Collider (LHC). This poster presents a study on the online High Level Trigger (HLT) system at CMS and its event selection performance on Vector Boson Fusion (VBF) Higgs production mechanism in Run3 of the LHC in the year of 2023 with integrated luminosity of $13\,\mathrm{fb}^{-1}$. Specifically, the efficiency study is done on the recently introduced event-level trigger paths characterized by the dijet invariant mass mjj and the relative pseudorapidity $\Delta\eta$ criteria of multijet events. 2023 Run3 SingleMuon datasets are employed with kinematic cuts applied on the transverse momentum of leading and sub-leading jets (pT_1, pT_2), mjj, and $\Delta\eta$ matching the trigger path algorithm, as well as calorimeter energy fractions and muon property cuts for well-defined event selection. With selected offline reconstructed events serving as the baseline, efficiency is obtained by taking the ratio of the number of events captured by VBF trigger paths to that of offline reconstructed events that are ideally accepted by the trigger path. Accurate and efficient performance of HLT on VBF trigger path will facilitate both the Standard Model studies and Beyond Standard Model (BSM) searches including Soft Unclustered Energy Pattern (SUEP) process.

F44: Developing SAXS Methodology for Solutions of Polystyrene Spheres. Collin P Douglas, Patrick Herron, Kiril A Streletzky (Cleveland State University)
Attempts to study solutions of hydroxypropyl cellulose (HPC) microgels using small angle x-ray scattering (SAXS) were performed at Kent State University's AMLCI lab to expand on and verify previous results from static and dynamic light scattering. However, the results gathered from our initial methodology did not reflect the results previously gathered nor made sense within the context of SAXS. From these issues an entirely new methodology for running and analyzing SAXS results needed to be created by adjusting parts of the initial methodology. By deciding to use water-based solutions of polystyrene microspheres (PS) with the same size range we were able to utilize a sample with a known size and shape to self-teach SAXS and introduce corrections to our methodology. To improve we needed to eliminate masking, match detector and distance settings to sample sizes, determine scaling factors and ranges, improve calibration procedures, and determine a fitting procedure in SASVIEW that accounts for program sensitivities. By taking a meticulous step-by-step approach to every part of our process we were able to improve our methodology and create a process that yields much more accurate and consistent results for the sizes of probes than what was initially utilized. We now plan to apply this methodology to HPC microgels in hopes of deducing their internal structure.

F45: High Altitude Re-entry Plasma Emulation Experiment (HARPEE). Ryan C Toonen, Christopher J Peters, Kerry J Johnson, Nicholas C Varaljay (Cleveland State University)
A table-top apparatus has recently been constructed at the NASA Glenn Research Center to investigate potential solutions for the *radio-frequency communication blackout* problem – experienced by landing modules during high-speed atmospheric entry. This customized plasma chamber was designed to emulate Earth-based atmospheric entry plasmas with electron densities in the range of 1016 m^{-3} to 1019 m^{-3}. The system makes use of a 40-kHz, perforated coaxial electrode pair to generate a disk-shaped, static plasma with an approximate diameter and thickness of 405 mm and 100 mm, respectively. A translatable Langmuir probe was employed to characterize the radial profile of electron temperature and density as a function the 40-kHz power ($< 1\,\mathrm{kW}$) and dry-nitrogen flow rate ($< 160\,\mathrm{SCCM}$).

F46: Optimizing the Exa.TrkX Inference Pipeline for Manycore CPUs. Alina Lazar (Youngstown State University)
The reconstruction of charged particle trajectories is an essential component to High-Energy Physics experiments. Recently proposed pipelines for track finding, built based on the Graph Neural Networks (GNNs), provide high reconstruction accuracy, but need to be optimized, in terms of speed, especially for online event filtering. Like other deep learning implementations, both the training and inference of particle tracking methods can be optimized to fully benefit from the GPU's parallelism ability. However, the inference of particle reconstruction could also benefit from multicore parallel processing on CPUs. In this context, it is imperative to explore the impact of the number of cores of a CPU on the speed related performance of running inference. Using both PyTorch and Facebook AI Similarity Search (Faiss) library multiple CPU threads capability combined with the weakly connected components algorithm result in faster latency times for the inference pipeline. This tracking pipeline based on the Graph Neural Networks (GNNs) is evaluated on multi-core Intel Xeon Gold 6148s Skylake and Intel Xeon 8268s Cascade Lake CPUs. Computational time are measured and compared using a range of different cores per task. The experiments show that the multi-core parallel execution outperforms the sequential one.

F47: Identifying Clumpy Galaxies: Insights from GALFIT and Non-Parametric Measurements. Abrar Khondker, Laura M DeGroot (College of Wooster)
This study focuses on the identification and investigation of clumpy galaxies in the Extended Groth Strip using GALFIT and nonparametric methods with James Webb Space Telescope data from the CEERS survey. Visual classification identified 108 clumpy galaxies, and a random sampling estimated approximately 48% of galaxies exhibit clumpy structures. GALFIT parametric decomposition showed most clumps are modeled by an exponential light distribution with an average Sersic index of n≈1, but some exhibited higher values up to 8.9, indicating a central concentration possibly related to massive black holes or increased star formation. This research aims to contribute valuable insight into the structural characteristics of clumpy galaxies, enhancing understanding of galaxy morphology and evolution.

F48: Advancing Atomic Modeling: Integration of Computational Clusters & Neural Network Techniques. Leonel Sanchez Torres (University of Mount Union)
High-precision atomic structure calculations require accurate modelling of electronic correlations involving large multielectron atomic structures. Here, we develop a deep-learning methodology that enables the preselection of the most pertinent configurations from huge basis sets until the desired precision is attained based on a weighted scale. Our approach performs under the control of a convolutional neural network that is being trained by previous GRASP examples. The findings for a number of cases involving numerous electron atoms demonstrate that deep learning can greatly reduce the amount of computer memory and processing time needed and makes large-scale calculations on previously inaccessible basis sets conceivable. Through the making of a cluster made of recycled Dell CPUs and the installation of the Linux operating system Rocky Linux 8.8 the cluster has the ability of preforming numerous GRASP examples which allow us to have confidence that the neural net is going to preform and were able to achieve our goal.

F49: Adsorbate Induced Resistivity Changes of Thin Au(111) films in Ultra High Vacuum. Dennis E Kuhl, Aaron Rohr, Kaitlyn Stewart (Marietta College)
Changes in resistance of a thin Au(111) film were measured using a four-probe, lock-in technique while dosing with diethyl disulfide. In a vacuum chamber with a base pressure of 2.5×10^{-10}Torr, the sample was sputter cleaned using Ar ions followed by an anneal cycle which heated the thin film to 500℃. The adsorbate-induced change in resistance was used to determine the fractional change in resistivity of the sample. Through multiple experiments the fractional change in resistivity was determined to be in the range of 0.019% ± .002% to 0.621% ± .002%.

F50: One-Dimensional Belousov-Zhabotinsky Chemical Wave System as an Electron Drift Analog. Augustus Thomas, Mahala Wanner, Niklas Manz (College of Wooster)
We use chemical reaction-diffusion (RD) waves in narrow channels to visually model electron drift velocity in a wire. By varying the initial conditions of an excitable Belousov-Zhabotinsky (BZ) system, we can create RD wave velocities in the range of typical electron drift speeds in conductors. The speed of the easily observable RD wave can then be compared with a theoretical electron drift velocity value to explore the effects of wire radius, current traveling through the wire, and the material composition. We present various chemical recipes to create desired electron drift velocities, providing a viable method for creating a visual aid to understanding electron drift velocity.

F51: Physics Fridays - Undergraduate Student Led Physics Outreach Program for K-12 Kids.. Patrick Herron, Jordan Miller, and Kiril A. Streletzky. (Cleveland State University)
In 2011 CSU's chapter of SPS established an outreach program called Physics Fridays. Since then, physics students & CSU physics alumni have gone to CIS once a month through the academic year for an interactive physics exploration session with CIS students. The outreach program has won 11 Marsh W. White Awards from the National SPS. These awards have supported a large part of the spring activities in the year-round program. We strive to create a variety of fun & exciting inquiry-based lesson plans to engage kids with physics/science. Since its inception, we have had more than 55 Physics Friday sessions at CIS, each consisting of three or four different demonstrations. Many of the outreach visits followed unique lesson plans, with no outreach session repeated more than 3 times. The lesson plans were created by an SPS outreach coordinator (we have been led by six excellent coordinators since 2011) & their team of volunteers. Since 2011, more than 50 CSU students have participated in Physics Fridays outreach lesson creation & execution along the way learning cool physics & quite a bit about themselves. This presentation will highlight our motivation & discuss the challenges & successes of our student-led physics outreach program.

F52: An Affordable Starter Lab for Intermediate Optics. Meimei Lai, Mark Fluegemann, Ernest R Behringer (Eastern Michigan University)
We have designed an affordable starter lab for intermediate optics aimed at measuring transmitted irradiance distributions generated by multiple LED sources of light when they illuminate centimeter-scale apertures. Students can explore a large parameter space by choosing the number and relative positions of the LEDs, different aperture shapes, and the relative positions of light sources, apertures, and screens. The lab can be extended using laser cutting, printed circuit design, and 3D printing tools, providing opportunities for further skill development. Additionally, image analysis tools can be employed to directly compare observations with the results of simulations available through a PICUP Exercise Set.

F53: Studying the most energetic explosions in the universe: Standard afterglow modeling of Gamma Ray Burst 050802. Gianlucas Sherrill Velarde (Eastern Michigan University)
Gamma-ray bursts (GRBs) are among the most energetic events in the universe, typically caused by the collision of supermassive objects and the collapse of very large stars. This can result in the ejection of very large quantities of matter and energy. The observed light from the remnants of these bursts, known as an afterglow, can be modeled according to the evolution of the brightness of each frequency of light as well as the type of environment that it travels through. We worked on modeling the afterglows of GRBs from the BAT6 sample, a collection of long duration GRBs with favorable observation conditions. We estimated and fitted physical parameters using inferences from the data and later running a Markov-Chain Monte-Carlo (MCMC) simulation to determine uncertainties on these parameters.In this work we present the analysis and standard afterglow modeling of GRB 050802. The UV and X-ray temporal data obtained from the SWIFT/UVOT telescopes show several nonstandard effects at early times. After this time the data can be fitted with a power law consistent with the available optical data. Additionally, we observed evidence of brightness contribution from the host galaxy of the GRB at later times. We use this knowledge to fit a slow cooling interstellar medium model, explained in this work. Together with other analyzed GRBs, this work will help develop and better understand GRB modeling techniques.

F54: Multidisciplinary REU site at Cleveland State University: Synthesis, Assembly, and Characterization of Soft Matter. Kiril A Streletzky, Jessica E Bickel (Cleveland State University)
Cleveland State University's NSF sponsored REU site on *Synthesis, Assembly and Characterization of Soft Matter Systems* is in the second 3-year period. The program is housed in the CSU's Physics Department but includes faculty from CSU's Physics, Math, Chemical & Biomedical Engineering and collaborators at Case Western Reserve University. The objective of our Soft Matter REU site is to involve undergraduate physics and engineering majors in meaningful interdisciplinary research projects within soft matter science and engineering focusing on the unique properties and applications of soft matter materials. A primary goal of our site is to encourage students to continue in STEM fields as either graduate students or workforce members. CSU's focus on Engaged Learning has cultivated a strong culture of support for undergraduate research, and REU participants benefit from this culture. Students receive one-on-one mentoring from experienced faculty and participate in a variety of professional development opportunities. The culture of collaborative multidisciplinary research at CSU would provide students with a unique perspective of working among peers and faculty from different academic disciplines. This poster will give an overview of the student research accomplishments and experiences from its first REU cycle. It will focus the benefits of the experience to both students and faculty mentors.

F55: Emissive nanoclusters in B4 helical nanofilaments for the next generation of polarized optics.. Marceline Myers, Jiao Liu, Jeanne Rebours, Ashwathanarayana Gowda, Yann Molard, Torsten Hegmann, Marianne E Prévôt (Kent State University)
The purpose of this study is to maximize circularly polarized luminescence with irradiated light utilizing chiral templating that manipulates the helical nature of bent core liquid crystals concentrated with a high quantum-yield dye. Using this new, all-inclusive model in lab, a polarized light source and control through the helical-type morphology of the template gives access to highly tunable circularly polarized light with excellent dissymmetry factor () enclosed within its own system which can aid in many optical processes or thermal-rate indicators. Using a chiral template and an achiral dye with excellent quantum yield, chirality can be transferred, thus resulting in a complex that can induce circular polarization without losing intensity through aggregation-caused quenching. Using Polarized Optical Microscopy and Circularly Polarized Luminescence instrumentation while fine tuning the weight concentrations of the Clustomesogen, confined within a variety of alignment layers within quartz cells, the luminescence dissymmetry factor of 0.55 was obtained with the maximum concentration of weight being 50%. To further strengthen the data for thermal applications, Differential Scanning Calorimetry data was collected and will lend information regarding helpful phase changes in these systems.

F56: Characterizing Pentacene Thin Film Growth on HOPG. Grace M Miller, Jessica E Bickel (Cleveland State University)
Organic electronics are generally more cost effective and environmentally friendly compared to their inorganic counterparts. However, organic materials often have an amorphous structure that makes them less conductive and less efficient in electronics. Their conductivities can be improved by creating crystalline films, which makes the distance between adjacent molecules uniform and allows for easier electron movement between adjacent molecules. One method for crystallizing organic materials is self-assembly on atomically ordered surfaces. In this work, Pentacene is thermally evaporated onto Highly Oriented Pyrolytic Graphite (HOPG) using a line-of-sight evaporation method. The resulting films are characterized by Scanning Tunneling Microscopy (STM) with the goal to determine ideal pentacene parameters for thin-film evaporation. While most trials tended to have disorganized depositions, we observed pentacene forming organized structures in two trials. In the first, we observed a honeycomb structure with a periodicity of 9.4 nm. We compared the unit cell spacing to the dimensions of both a single pentacene molecule and pentacene's general triclinic crystal structure but neither fit our sample. A second organized trial showed a slightly smaller repeating pattern along a step edge with a spacing of 4.4 nm. While not crystalline, this structure was periodic in the single dimension of the step edge. This structure was only compared to a single pentacene molecule, as the structure was a similar height to a monolayer of pentacene, but again the values do not quite match our structure. We were unable to reproduce either of these trials, largely due to our Quartz Crystal Monitor (QCM) giving inaccurate growth rates and thicknesses. Being able to reproduce these structures and determine more refined deposition parameters for which they form is essential to learn more about how pentacene is forming on the substrate. While we were unable to determine exactly how the pentacene molecules were forming on the substrate, our work shows pentacene's ability to form organized structures.

F57: Fundamental Properties of Three Metal-Poor Stars with Optical/NIR Interferometry. Eliot G Hiegel, Tabetha S Boyajian, Ashley Elliott (Denison University)

Angular diameters of three metal-poor and one solar metallicity star-HD 184499, HD 22879, and HD 76932 and HD 108510-were measured using the CHARA Array interferometer. Angular diameters θLD = 0.403 ± 0.004, 0.397 ± 0.006, 0.570 ± 0.005, and 0.360 ± 0.006 mas were found for HD 184499, HD 22879, HD 76932, and HD 108510, respectively. Using these diameters combined with Hipparcos parallaxes and literature values for bolometric flux, linear radii R = 1.38 ± 0.02, 1.09 ± 0.02, 1.29 ± 0.01, and 1.16 ± 0.03 R_0; effective temperatures $T_{\rm eff}$ = 5824 ± 47, 5856 ± 50, 5913 ± 47, and 5950 ± 84 K; and luminosities L = 1.97 ± 0.07, 1.26 ± 0.04, 1.82 ± 0.05, and 1.50 ± 0.09 L_0 were calculated. Given these values along with literature values for [Fe/H], the Python package Kīauhōkū was used to compute an age and mass for each star from four stellar model grids. For the metal-poor stars, the resulting ages were higher than literature values and the masses lower. For the HD 108510, the resulting ages were higher than literature values while the masses agreed. To investigate the discrepancies in age, all four stars were fitted to DSEP isochrones, accounting for alpha-enhancement in the three metal-poor stars. The resulting fits indicated significantly lower ages than those computed by the model grids for the metal-poor stars and an age for HD 108510 which agreed with the model grids.

Contributed Talks: Sessions L1-L5 (SI 117, 118, 147, 148, & 149)

Session L1: Material Science, Computational Physics and Data Science
Room SI-117. Session Chair: Dr. Dennis Kuhl (Marietta College)

L1.1: Revealing Microdynamics that Underlie Tire Tread Performance. Hakan Aras (University of Akron)
Filled elastomers are used in many applications, including tire tread. Functionalized chain additives and coupling agents have been used to enhance interactions between filler and polymer matrix in silica-filled styrene butadiene rubber (SBR). These interactions create bound polymer layers around the filler that alter the dynamic performance by changing aggregate size and connections among particles, forming strong 'force chains'.We have synthesized well-defined functionalized polymeric chain additives and nonfunctional analogs to probe how changing the filler/polymer interface chemistry changes the filler microscopic response and thus the macrodynamics. This study spans length scales from that of the networked agglomerates to that of filler/polymer interfaces. We probe the filler network's microscopic response using X-ray Photon Correlation Spectroscopy (XPCS) while the sample is under oscillatory strain. The rate of change in the intensity-intensity time autocorrelation during the measurement provides information on the filler network microdynamics. The microscopic responses of samples containing functionalized chain additives differ from those of samples containing nonfunctional additives.

L1.2: Structural and Optoelectronic Characterization of AgSbI4 through Machine Learning and Density Functional Theory. Chinmay Khare (University of Toledo)
Lead-free metal halides, as emerging materials for photovoltaic and optoelectronic applications, have garnered substantial attention, especially given the increasing global emphasis on environmental sustainability. AgSbI4 is an example of such a material that has recently been synthesized and shows intriguing characteristics but has not yet been adequately explored with density functional theory due to its pronounced site-disorder in its cation sublattice. We harness the potential of a kernel ridge regression machine learning model of the total energy in AgSbI4 to choose a few simulation cells out of 107 possibilities; a task out of reach for current *first principles* techniques. With these models, we calculate structural and optoelectronic properties ranging from X-ray diffraction patterns to absorption and reflection spectra. We compare these results with existing experimental data, for example, the average band gap of 1.96 eV, and lattice constants (a, c = 4.4, 21.0 Å). We calculate effective masses (⟨m*e⟩ = 0.4 m0 and ⟨m*h⟩ = 4.1 m_0), bulk modulus (35 GPa), and formation energies with respect to AgI and SbI_3 (50 meV per formula unit). We analyze the density of states, use LOBSTER to calculate Crystal Orbital Hamilton Populations, and perform Bader charge analysis to compute charge transfer. Significantly, our predictions concerning optoelectronic properties indicate AgSbI4's potential as an absorber layer in next-generation tandem photovoltaic cells.

L1.3: Trions in Monolayer MoS2 using Faddeev Scheme in Momentum Space. Mohammadreza Hadizadeh (Central State University)
In this presentation, we study the binding energy and geometrical structure of negative trions, the bound state of two electrons and one hole interacting via the Rytova-Keldysh interaction in Monolayer MoS_2. We introduce a general framework developed in momentum space for the bound state of three different charged particles, interacting with distinct interactions in two dimensions. We discuss the numerical challenges and their solutions for handling repulsive electron-electron interaction when solving the coupled Faddeev integral equations and calculating the trion's binding energy and wave function.

L1.4: Temperature Replica Exchange Gaussian Accelerated Molecular Dynamics: Improved Enhanced Sampling and Energetic Reweighting. Timothy Hasse (Wayne State University)
Gaussian accelerated molecular dynamics (GaMD) provides enhanced sampling and energy reweighting of biomolecules. GaMD works through adding a harmonic boost potential, defined by a force constant and a threshold energy, to smooth the potential energy surface and accelerate sampling between different states of a biomolecular system separated by large energy barriers. Previously, GaMD has been combined with replica exchange algorithms to improve the acceleration power and energy reweighting of the conventional GaMD simulation. Replica exchange GaMD (Rex-GaMD) comes in two varieties: force constant Rex-GaMD and threshold energy Rex-GaMD, which exchange between replicas of different harmonic force constants and threshold energies, respectively. Recently, Rex-GaMD has been combined with the parallel tempering algorithm that exchanges replicas which vary over a range of temperatures. This new method of temperature Rex-GaMD (T-Rex-GaMD) is able to exchange any combination of replicas defined over a range of different values of the force constant, energy threshold, and temperature. Our hope is that the use of high temperature replicas, in addition to force constant and energy threshold replicas, will lead to accelerated sampling of interesting biomolecular systems with multiple different conformational states separated by large energy barriers. For this new method to be useful we must still be able to perform accurate energetic reweighting, allowing us to recover the true free energy profile of our biomolecular system. To this date, we have performed T-Rex-GaMD simulations on three test systems: alanine dipeptide, chignolin, and HIV protease.

L1.5: Invariance in Deep Network Learning: Mathematical Representation, Probabilistic Symmetry, Variable Exchangeability, and Sufficient Statistics. Yueyang. Shen (University of Michigan)
Algebraic Lie groups provide the foundation for describing many physical symmetries, which play a key role in studying the geometry of smooth manifolds and analyzing complex high-dimensional observations. In particular, Noether's symmetries articulate the correspondence between physical symmetries and conservation quantities, which often correspond to physical laws that can be prescribed as differential equations. This interplay between mechanical dynamics, symmetries, information, and geometry characterizes the importance of Lie group actions on modeling classical physical systems, obtaining rigorous statistical inference, and training of deep artificial intelligence (AI) networks. Lie group characterize data symmetries in the underlying learning problems. Classical machine learning approaches for examining symmetries include data augmentation (data-driven) and architectural modifications to construct invariant models through weight constraint designs (model-based). A model-based G-invariant design often composed several equivariant functions followed by a final invariant function. A concurrent work suggests that building group invariance and partial invariance into string theory Kreuzer Skarke dataset improve model performance. Non group invariant models benefit from group invariant preprocessing.From a statistical point of view, classical symmetry is related to probabilistic distributional symmetry, where exchangeability and stationarity are the primary examples. For instance, a sufficient sample statistic contains all the information needed for an inferential procedure and is directly related to probabilistic symmetry. That is, sufficiency describes the information that is relevant to the statistical inference. Probabilistic symmetry and invariance identify information that is irrelevant to the statistical inference. In this talk, we will review and investigate the relations between mathematical invariance, DNN invariants, (probabilistic) symmetries, physical modeling, PDE solutions, geometries and information.

L1.6: Influences of Blood Flow Waveform Uncertainties on Computational Hemodynamic Evaluation for Intracranial Aneurysms. Hang Yi (Wright State University)
Boundary condition (BC) is one of the most critical factors in the accuracy of hemodynamic evaluations of intracranial aneurysms (IAs) using computational fluid dynamics (CFD) modeling. Most previous investigations used a uniform rather than the patient-specific physiological blood flow waveform as BCs for numerical modeling of IAs, which could induce significant errors in risk evaluations and lead to wrong diagnoses for patients with IA symptoms. To secure the prime BC for hemodynamic modeling for IAs and quantify the hemodynamic differences under various BC strategies, this study conducted a comprehensive investigation based on Doppler ultrasound measurements and the discrete Fourier transform (DFT) simulation. First, the periodically pulsatile blood velocity at the internal carotid artery (ICA) was measured by the ultrasound flowmeter for the IA patient with a heart rate of 57 Hz, which was plotted and then phase-averaged as the baseline physiological BC for CFD modeling. Subsequently, the number of discrete points, i.e., N = 8, 16, 22, 36, and 106 on the phase-averaged waveform, were employed to generate five simulated waveforms as BCs for CFD modeling by comparing agreements in hemodynamics with the phase-averaged scenario. In addition, hemodynamic performances under the patient-specific physiological BC and a previously employed uniform BC were compared to check the errors induced by the uniform waveform assumption. The preliminary results showed that more discrete points are selected for a DFT waveform, better agreements in hemodynamics (i.e., maximum wall shear stress (WSS), surface-averaged (SA-WSS), oscillatory shear index (OSI)) on the IA sac wall can be obtained. It results in the correlation coefficients of 0.94, 0.98, 0.993, 0.996, and 0.998 under scenarios of N = 8, 16, 22, 36, and 106, respectively. It suggests that N = 22 are acceptable prime DFT points to generate a BC for hemodynamic modeling by considering the balance of modeling accuracy and DFT complexity. Additionally, significant differences in hemodynamics resulting from uniform and patient-specific BCs suggest the latter is essential to ensure the accuracy of hemodynamic predictions for IAs.

Session L2: Physics Education Research and Educational Tools, Theoretical Physics
Room SI-118. Session Chair: Dr. Ernest Behringer (Eastern Michigan University)

L2.1: Theoretical physics laboratory: a scaffolded active learning approach for upper year physics courses. Mark Baker (Rose-Hulman Institute of Technology)
Due to low enrollment sizes and infrequent course offerings, specialized upper year theoretical physics courses have few studies which have been completed in the physics education research literature. Such courses are conventionally delivered in a strict didactic form, where the instructor delivers 3 independent hour-long lectures per week. Students are often left to work through the related highly complex and lengthy derivations independently, many times avoiding them altogether as they are difficult to incorporate and therefore not emphasized in standard didactic course assessments. To help address this gap we developed a course and physics education research proposal in 2021, a course which we were able to offer and complete the corresponding research study in 2023. In this course we take several approaches which are supported by the education literature, in particular focusing on scaffolded active learning during a single lengthy session, once per week. The single meeting is designed similar to laboratory based learning for experimental courses, and is modeled after popular 'escape-rooms', where students must work together to finish a flexible list of tasks. Results from the study provide strong evidence for this course method to be incorporated into upper year physics course offerings. In our presentation we will discuss the course design, research study and results, instructional methodologies, and related literature. We will also provide some sample teaching materials and demonstrate the basic function of the weekly session of the course.

L2.2: Career Readiness for Physics Students (and Faculty): APrésumé Program. Charlotte Bimson (Case Western Reserve University)
We present the results of a campaign to improve physics undergraduate and graduate career awareness and development. Students are unaware of possible nonacademic career paths-specifically in industry-and have limited knowledge of populating a strong, job-focused resume. To tackle this issue, we created a seminar course where a series of industrial physics talked about their career path. It is important to emphasize that the class did not dissuade students from academia but created opportunities to prepare for *all* career paths. The proposal is made based on the results of the course. We suggest that student advisors take a more vital role in preparing physics students for various careers: being aware of the career probabilities for a physics bachelor, encouraging electives and internships outside of physics to build a diverse background, and continuously building the students' resume and cover letters. The focus is on the latter. We suggest that all physics students, as they progress academically, should create practice resumes: a pre-résumé or a présumé for short (with accent marks for pronunciation). We propose a program presuming early students should have a présumé: The physics présumé program.

L2.3: ChatGPT Takes Physics Exam. Brian Woodahl (Indiana University–Purdue University Indianapolis)
Can ChatGPT help students learn introductory physics? How can we incorporate ChatGPT into our physics recitations? To illustrate the importance of ChatGPT, this past spring semester, ChatGPT took one of my exams in the first semester, algebra-based physics course on mechanics. I discuss how it performed, compare its score to the rest of the class (humans) and discuss how ChatGPT (Chat Generative Pretrained Transformer) has the potential to dramatically change the landscape in introductory physics courses.

L2.4: Newton's Off-center Circular Orbits and the Magnetic Monopole. Dipesh Bhandari (Texas A&M University - Commerce)
Introducing a magnetic field into Newton's off-center circular orbits potential in such way as to preserve the $E = 0$ dynamical symmetry leads to a unique choice that can be identified as the inclusion of a magnetic monopole in the inverse stereographically projected problem. One finds also a phenomenological correspondence with that of the linearly damped Kepler model. The presence of the monopole field deforms the symmetry algebra by a central extension, and the quantum mechanical version of this algebra reveals a number of zero modes equal to that counted using the index theorem of elliptic operators.

L2.5: Slowly-Rotating Q-Balls. Fabrizio Vassallo (Denison University)
Q-balls, soliton solutions in classical field theory, have wide-ranging applications, including in various theories of dark matter and baryogenesis. Although Q-balls with nonzero angular momentum are proven to be present in some of these theories, only solutions with quantized angular momentum are currently known. This work seeks to understand if other rotating solutions are possible.

L2.6: Electromagnetically Induced Transparency (EIT) and the Big Bang: The Sakharov Conditions on a table top. Victoria Thomas (Youngstown State University)

The Sakharov conditions met in the early universe may explain the matter-antimatter asymmetry of our universe. Chirped Zeeman EIT is an ideal optical analogue of the charge conjugation violation and universe expansion rate that satisfy the Sakharov conditions back then. We describe our experiment in warm 87Rb vapor and explain its findings in light of the quantum optics theory model. This enlarges the applicability and draws attention to the universal behavior of other physical processes that generalize the Sakharov conditions.

Session L3: Biophysics, Astrophysics and Space Science
Room SI-147. Session Chair: Dr. Laura DeGroot (College of Wooster)

L3.1: Exploring Mechanically-Induced Signaling in Kidney Epithelial Tissue: A Dual-Sided Perfused Flow Chamber Approach for Extended Cell Culture and Cellular Response. Ishan Chawan (Cleveland State University)
Our lab uses cultured kidney epithelial tissue to better understand mechanically-induced signalling in ciliated epithelial cells. In the fields of cell & tissue physiology, epithelial and endothelial cells can be studied using a perfused flow chamber ('FC') which 1) allows researchers to investigate the direct effects of bulk shear stress on intact tissue and 2) mimics a physiologically relevant environment for cultured tissue. However, cell/tissue culture within the confined volume of a fluid chamber introduces numerous complications compared to 'classical' cell/tissue culture in petri dishes. For example, there is an absence of standard protocols to help grow cells, and the small volumes of media requires more attention be paid to the buildup of excreted metabolic byproducts. In addition, there are complex operational control and FC design requirements. We are designing a dual sided FC where cells are plated and grow on a semi-permeable membrane, allowing epithelial tissue to perform its function as a selective transporter of material into and out of the organ(ism). Because the tissue culture is exposed to medial on both sides (apical and basolateral), we have the option to expose the tissue to 2 different kinds of media (for example, a blood side and an ultrafiltrate side). In addition, as it is dual sided we have independent control over the fluid flow on apical and basolateral sides, allowing us to record cellular responses to a range of different fluid flow patterns.I will present the work I have done to date, showing how we can now culture cells within a flow chamber for many days, and also demonstrate some of the experimental techniques we will use to characterize cell responses.

L3.2: The Relative Contributions of Neurofilament Gene Expression and Neurofilament Transport in Axonal Caliber Growth. Rawan Rawan (Ohio University)
During the postnatal stage of mammalian development, the myelinated axon expands radially until it reaches a target caliber that influences axonal conduction velocity and in turn neuronal function. Hence, the growth of axon caliber is an important developmental process to understand. This radial growth is mainly driven by an accumulation of neurofilaments (NFs), which are cytoskeletal polymers known for their space-filling role in axons. They are assembled in the neuronal cell body and transported into the axon along microtubules (MTs). The growth of axonal caliber is accompanied by an increase in NF gene expression and a decrease in NF transport velocity along the axon, but the relative contributions of these processes to the growth are not known. Guided by published data on axonal area, NF and MT densities as well as NF transport kinetics in vivo, we address this question by computational modeling of the growth of myelinated motor axons in rats. We find that the radial growth of these axons is mainly driven by an increase in NF influx at the earlier stages of development and by the slowing of NF transport at later times. We conclude that a decline in MT density provides a mechanism for the observed slowing.

L3.3: The Kraft Break Sharply Divides Low Mass and Intermediate Mass Stars. Alexa Beyer (Youngstown State University)
Main sequence stars are known to transition at mid-F spectral types from being slowly rotating (cooler stars) to being rapidly rotating (hotter stars), a transition known as the Kraft Break (Kraft1967) and attributed to the disappearance of the outer convective zone, causing magnetic braking to become ineffective. To investigate this Break more precisely, we assembled Gaia DR3 data and spectroscopic measurements of 405 F stars within 33.33 pc of the Sun. The Break boundaries occur at spectral types F4 and F5, effective temperatures of 6650 K and 6500 K, respectively. Using mass-temperature relations of eclipsing binaries, the Break boundaries correspond to stellar masses of 1.35 Msol and 1.28 Msol, Magnetic braking appears to become ineffective with only a small change in effective temperature and stellar mass. A study of F stars in the 625 Myr Hyades cluster shows that the Break is nearly but not fully established by this age; we speculate that it should be established in populations older than 1 Gyr. We propose that the Kraft Break provides a less ambiguous division between low mass stars and intermediate mass stars. The Break is observationally well-defined and is physically linked to a change in stellar structure.

L3.4: Spatially Resolved Stellar Populations of z 4 - 6 Lyman-alpha-emitting Galaxies with CEERS JWST NIRCam Imaging Turaba Rahman (Kent State University)
We perform a spatially-resolved stellar population study of Lyman-alpha emitters (LAEs) at z 4 - 6 in the Cosmic Evolution Early Release Science Survey (CEERS) field, that have been spectroscopically confirmed through ground-based observations. We use publicly available, deep, high spatial-resolution imaging data from the JWST NIRCam and HST observations to conduct spatially-resolved spectral energy distribution (SED) modeling. We analyze the radial variations of galaxy properties through our spatially-resolved SED fitting to address key questions: when/where these galaxies form stars actively, and what physical mechanisms regulate star formation. Finally, we learn about the enhanced star-formation rates near the galactic centers and examine trends in stellar mass surface density, stellar metallicity, dust attenuation, and mass-weighted age.

L3.5: An Angular Diameter Measurement of β UMa with Stellar Intensity Interferometry at VERITAS. Josephine Rose (Ohio State University)
In this talk, I will present a measurement of the angular diameter of β UMa, the first scientific stellar intensity interferometry result from VERITAS, including results of an upcoming paper and details of observations and the analysis. VERITAS (Very Energetic Radiation Imaging Telescope Array System) is an array of four IACTs (Imaging Air Cherenkov Telescopes) used primarily for ultra high energy gamma ray astronomy. VERITAS stellar intensity interferometry exploits the bright period around the full moon to measure stars at a visual wavelength of 416 nm, with six pairs of telescopes providing a range of baselines approximately 35-170 m. SII is based on the Hanbury-Brown Twiss (HBT) effect, which is a part per million increase in probability in the product of the intensities of correlated light at the same relative time. The relationship between time correlations of the intensities of light between pairs of telescopes and their projected separation are used to produce a wavelength-dependent measurement of the angular diameter of a star. From nearly 40 hours of observations, we have measured the uniform disk angular diameter of &β; UMa to be 1.01 ± 0.03 mas. We also calculate the limb-darkened angular diameter of the star to be 1.06 ± 0.04 mas, to compare to previous measurements from other observatories at different wavelengths. I will discuss steps of the data analysis, including removal of contaminating frequencies, time-shifting of the correlation function to account for the change in optical path delay as the star travels across the sky, and time averaging to produce a correlation function, as well as the scientific importance of this measurement.

L3.6: How MOND-like is Quasilinear MOND? Investigating the Vertical Acceleration Field of the Milky Way. Sofia Splawska (Carnegie Mellon University)
The mass discrepancy problem is a long-standing, unresolved problem in astronomy with possible consequences in many areas of physics. The problem refers to an inconsistency between the amount of observed mass in the universe and its dynamics as predicted by our best theory of gravity, General Relativity. Two proposed solutions to this problem are the dark matter paradigm, which is standard, and MOdified Newtonian Dynamics (MOND), a modification to Newtonian gravity at low accelerations which has been less studied. Both hypotheses have multiple problems and neither has been ruled out. Notably, a direct detection of dark matter is still lacking. Therefore, there is a need to test the validity of both theories. The vertical acceleration field of disk galaxies can provide a sharp test to distinguish between MOND and Dark Matter. We propose a test of MOND vs dark matter using the vertical acceleration of the Milky Way calculated from local observables. Previous work found that MOND is disfavored relative to Dark Matter due to an overprediction of the Milky Way's vertical acceleration compared to observations, but in this work the physically inconsistent pristine MOND was used as a proxy for all MOND-like theories. Here we explore whether the tension with Milky Way data exists with the Quasilinear MOND (QUMOND). We develop a QUMOND Poisson solver using Fourier methods, and use it to compare the vertical acceleration fields in exponential disk galaxies with the pristine MOND prediction. Our results have the potential to provide evidence for MOND in the Milky Way or against it.

Session L4: Applied and Engineering Physics, Condensed Matter Physics, Chemical Physics
Room SI-148. Session Chair: Dr. Niklas Manz (College of Wooster)

L4.1: Analysis of Thermoradiative Thermal Energy Conversion. Geoffrey Landis (NASA John H. Glenn Research Center)
The thermoradiative cell is a new method for converting heat energy to electrical power, first detailed by Strandberg in 2015. The cell is a p-n junction semiconductor device, similar to a photovoltaic cell but thermodynamically operating in the reverse direction, converting the thermal dark current into electrical power while radiating waste heat to space.The power and efficiency can be calculated as a function of bandgap in the Shockley-Queisser detailed-balance limit, in which the thermal emissivity of the cell is due to the recombination of electron-hole pairs, and all other recombination losses are ignored. The current produced is directly proportional to the recombination radiation. The fundamental loss mechanism for the thermoradiative cell is the energy carried by the infrared radiation into space from band-to-band recombination of carriers injected across the junction. In an ideal cell, to maximize the efficiency, the emission energy of these photons would precisely equal the bandgap. This can be achieved, for example, using dielectric filters or meta-material filters to recycle emission at other wavelengths back into the cell.The voltage is proportional to the external bias. These two constraints allow optimization of the optimum bias point for maximum power. Unlike photovoltaic cells, the maximum power operating point is not the same as the maximum efficiency point, and higher efficiency can be achieved at a higher (negative) bias in the ideal case. Incorporating non-ideal losses, however, shifts the maximum efficiency point toward lower bias. Unlike in photovoltaic cells, non-radiative recombination (e.g., Auger losses) will reduce the output current, but will not reduce the conversion efficiency, since the recombination energy is retained in the cell in the form of heat.Since a thermoradiative cell operates by radiating directly to space, the current produced by themoradiative cells will increase as Stefan-Boltzmann radiation; roughly the fourth power of the temperature. Thus, the power produced is highest at high operating temperatures, and, unlike conventional thermal conversion, increasing radiator temperature increases, the efficiency. Thus, the choice of technology will be toward semiconductors resistant to degradation at high temperature.

L4.2: Reentrant fractional quantum Hall state: A charge ordered and broken symmetry phase of composite fermion. Haoyun Huang (Purdue University)
Non-interacting composite fermions can be used to account for the majority of fractional quantum Hall states. However, the residual interactions between composite fermions can lead to the formations of more exotic states with complex correlations. We recently observed a bubble phase of composite fermions in a GaAs two-dimensional electron gas sample near Landau level filling factor $\nu = 5/3$. This phase with very interesting correlations was identified via a reentrant behavior of the fractional quantum Hall effect in transport measurements. Our finding reveals a new class of strongly correlated topological phases, driven by the clustering and charge ordering of emergent quasiparticles.

L4.3: Single particle and collective localization around ν=1 integer quantum hall plateau in a high mobility two-dimensional electron system. Waseem Hussain (Purdue University)
In a two-dimensional electron system, different topologically protected bulk orders can occur depending upon the competition between electron-electron interaction and the disorder potential. In the middle of $\nu = 1$ plateau the bulk corresponds to single particle localization, Anderson Insulator, whereas the flanks correspond to a periodic arrangement. This type of localization corresponds to the appearance of Wigner crystal known as Integer Quantum Hall Wigner Solid (IQHWS). The phase boundaries of these states and other properties will be discussed as obtained from transport measurements in modern GaAs samples.

L4.4: 2D semiconductor FETs: the role of flake vs dielectric thickness Xiaotong Li (Case Western Reserve University)
Layered semiconductors are being actively studied for their possible application in high-performance field effect transistors (FETs). While transistors made of 2D semiconductors have been realized, the effect of their thickness on device performance is not fully understood. Moreover, the validity of conventional metal-oxide-semiconductor (MOS) equations on these 2D device structures is a topic of great interest. In this paper, we examine the role of 2D semiconductor flake and oxide dielectric thickness in the determination of the subthreshold swing of WSe_2 FETs. By extracting the subthreshold swing of various devices with different flake and oxide thicknesses, and comparing it to the subthreshold swing expression derived from MOSFET theory when the semiconductor thickness is used as the depletion width, we are able to validate the use of such equation for the determination of the subthreshold swing in 2D semiconductor FETs. Additionally, we explore how the oxide and semiconductor thicknesses affect the determination of the threshold voltage.

L4.5: Topological transitions induced by strain in the kagome lattice. Miguel Mojarro Ramirez (Ohio University)
We study the effects of a uniform strain on the electronic and topological properties of the 2D kagome lattice using a tight-binding formalism that includes intrinsic and Rashba spin-orbit coupling (SOC). The degeneracy at the Γ point, where a flat-band-parabolic-band touching occurs, evolves into a pair of (tilted) type-I Dirac cones owing to a uniform strain, as shown by effective Hamiltonians, where the anisotropy and tilting of the bands depend on the magnitude and direction of the strain field. Interestingly, we find that the Dirac cones become type-III (including flat dispersions) when the strain is applied along the bonds of the lattice. As expected, the inclusion of intrinsic SOC opens a gap at the emergent Dirac points, making the strained flat band topological, as characterized by a nontrivial Z2 index. We show that the strain drives the systems into a trivial or topological phase for strains of a few percent, allowing topological transitions via uniform deformations. Additionally, when the Rashba interaction is included, semimetallic phases appear in the topological phase diagrams. These findings suggest an alternative way of engineering anisotropic tilted Dirac bands with tunable topological properties in strained kagome lattices.

L4.6: Visualization of orbital free models of the kinetic energy density in semiconductors. Antonio Cancio (Ball State University)
Meta-generalized gradient approximations (mGGAs) for the exchange-correlation (XC) energy in density functional theory (DFT) conventionally depend upon the Kohn-Sham kinetic energy density (KED). Use of the KED makes mGGAs more accurate than generalized gradient approximations (GGAs) but also more computationally expensive for applications such as ab initio molecular dynamics. Deorbitalizated mGGAs replace the KED with a pure density functional. Through visualization we explore how well the exact KED can be represented by a single KE mGGA functional dependent upon the scaled density, scaled density gradient and density Laplacian. We calculate the KE and electron density of semiconductor solids with varying ionicity and atomic number using the ABINIT DFT plane-wave pseudopotential code. We find a near-universal linear correlation with the density Laplacian and density gradient for regions outside the atomic bond, consistent with a modification of the second-order gradient expansion. Non-self-consistent calculations of structural properties such as the lattice constant and bulk modulus, using various approximate KED functionals, were performed. We find best performance of mGGA KED models for those that best approximate the observed linear correlation.

Session L5: Optics, Photonics, and Spectroscopy, Nuclear and Particle Physics
Room SI-149. Session Chair: Dr. Petru Fodor (Cleveland State University)

L5.1: Electrochemical Bubble Delamination and Transfer of CVD Graphene from Copper to Si/SiO_2 Utilizing Mechanical Assistance. Zane Perrico (Youngstown State University)
High quality graphene can efficiently be grown on large surface areas of copper foil through chemical vapor deposition (CVD). To transfer CVD graphene onto a substrate for use in nanoscale photonic devices a process called electrochemical bubble delamination is utilized. During the delamination and transfer procedure the CVD graphene is at its most susceptible. Therefore, the incentive to develop a minimal-contact and replicable process is high. The use of a mechanical stage controlled by an actuator is a promising method of avoiding significant mechanical defects like folding or tearing and is capable of ensuring the film is delaminated at the right speed and from bottom to top. The quality of the transferred graphene is varied with regions of high-quality graphene up to 80x80µm while the typical transfer region has a large presence of gaps, cracks, and PMMA residues. It is evident that extending the mechanical assistance to other parts of the transfer process may be valuable, however, the occurrence of mechanical and chemical defects in the transferred graphene is still a limiting factor in the use of electrochemical bubble delamination.

L5.2: Study net proton fluctuations with (3+1)D hybrid simulations and machine learning. Brandon Boudreaux (Wayne State University)
Numerical simulations of the (3+1)D hydrodynamic + hadronic transport hybrid model provide quantitative descriptions of the dynamics of relativistic heavy-ion collisions from a few GeV to a few TeV [1]. The net proton cumulants in the final state encode important information about the QCD phase structure. However, studying high-order cumulants of net proton fluctuations require more than millions of simulation events, which poses a big computational challenge. In this work, we develop a neural network to mimic the net baryon charge evolution in the full (3+1)D hybrid model. The trained neural network enables us to efficiently compute the net proton cumulants. Based on the trained neural network, we study the net proton cumulants from fluctuations of initial-state baryon stopping modeled by the 3D Monte-Carlo Glauber model at the RHIC Beam Energy Scan energies.[1] C. Shen and B. Schenke, 'Longitudinal dynamics and particle production in relativistic nuclear collisions,' Phys. Rev. C 105, no.6, 064905 (2022).

L5.3: Quasielastic Electron-Nucleus Scattering and the Correlated Fermi Gas Model. Sam Carey (Wayne State University)
The study of neutrino-nucleus scattering processes is important for the successful execution of the entire new generation of neutrino experiments like DUNE and T2K. Quasielastic neutrino-nucleus scattering, which yields a final state consisting of a nucleon and charged lepton, makes up a large part of the total neutrino cross-section in neutrino experiments. A significant source of uncertainty in the cross-section comes from limitations in our knowledge of nuclear effects in the scattering process. To this end, electron-nucleus scattering experiments play an important role in providing vital information to test and validate different nuclear models intended to be used in neutrino experiments. We present a cross-section calculation for the lepton (electron and neutrino) nucleus quasielastic scattering process using the Correlated Fermi Gas nuclear model characterized by a depleted Fermi gas region and a correlated high-momentum tail. This is carried out by identifying various transitions available for the nucleon inside the nucleus and thereby calculating the corresponding phase-space integrals for the nuclear structure tensor. We discuss the comparison between cross-sections from this model with the available experimental data and the widely used Relativistic Fermi Gas (RFG) nuclear model.

L5.4: Separable Non-Local One-Body Ground State Densities for light 0+ Nuclei. Joseph Foy (Ohio University)
Nucleon-nucleon (NN) interaction potentials derived from Chiral Effective Field Theory used in conjunction with the no-core shell-model (NCSM) allows *ab initio* predictions of light nuclei structure and scattering observables. In a multipole expansion of the non-local one-body density matrix (OBDM), nuclei with 0+ ground states are completely described by the monopole term. It is advantageous to consider these OBDMs in momentum space, specifically where the momentum transfer and the average momentum are the coordinates.We investigate the dependence on the angle between those two momentum vectors for OBDMs for s- and p-shell nuclei (^{4}He, ^{12}C, and ^{16}O) derived in the NCSM framework from different chiral NN interactions. We find that those OBDMs are separable in the chosen momentum variables. However, OBDMs in terms of the initial and final momentum (p,p') exhibit dependence on the angle between them.

L5.5: Laser-Driven Table-Top Accelerator Facility to Generate kHz-rate Mixed Radiation. Benjamin Knight (Air Force Institute of Technology)
High-repetition-rate energetic electrons, protons, x-rays and neutrons are generated at AFIT's Extreme Light Laboratory (ELL). The extremely high intensity laser pulses bombarded on the unique homegrown liquid target enables such mixed radiation detection.

L5.6: Wolfenstein Amplitudes Derived from a Chiral NN Interaction up to N4LO. Bradley McClung (Ohio University)
Chiral nucleon-nucleon (NN) interactions are successful at describing two and three nucleon forces, and in the two-nucleon sector their constants are fitted to NN observables. This talk focuses on the Epelbaum-Krebs-Meissner (EKM) NN interaction with a local coordinate-space regulator. From a given NN interaction, one usually calculates phase shifts, which are then used to determine scattering observables. An intermediate step is to construct Wolfenstein amplitudes from the phase shifts, which may allow to investigate their connection to the operator structure of the NN interaction. In this talk, the Wolfenstein amplitudes and their dependence on the NN laboratory energy up to 200 MeV as well as the cutoff parameter will be shown. Furthermore, the contributions of the different partial waves to each amplitude will be investigated.

APS EGLS Leadership and Service: 2023-2024

Chair: Bhubanjyoti Bhattacharya	*bbhattach@ltu.edu*
Chair-Elect: Zifeng Yang	*zifeng.yang@wright.edu*
Vice Chair: Ronald J Tackett	*rtackett@kettering.edu*
Past Chair: Niklas Manz	*nmanz@wooster.edu*
Treasurer: Donald J Priour	*djpriour@ysu.edu*
Secretary: Rachel J Henderson	*hende473@msu.edu*
Assigned Council Representative: Nadia Fomin	*nfomin@utk.edu*
Member-at-Large: Edward Carlo C Samson	*samsonec@MiamiOH.edu*
Member-at-Large: Ronald E Kumon	*rkumon@kettering.edu*
Student Member: Jacob Jeffrey Callebs	*jcallebs24@wayne.edu*

Society of Physics Students Zone 7 Meeting - Program Outline

Friday October 20

2:15 - 2:45	SPS Registration - Fenn Tower Atrium
2:45 - 3:00	Welcome - Fenn Tower 303 **Dr. Andrew Kersten**, Dean, College of Arts and Sciences, CSU
3:00 - 3:45	**SPS Zone 7 Meeting Kick-off** - Fenn Tower 102 CSU SPS Officers, Dr. Ronald Kumon, Jacob Callebs, Dr. Kiril Streletzky. Undergraduate students, please come to introduce yourself
3:45 - 4:00	Coffee Break
4:00 - 4:45	Synthetic DNA Nanostructures as Platforms for Precise Nanoparticle Organization **Dr. Divita Mathur**, Case Western Reserve University - Fenn Tower 303
4:45 - 5:00	Coffee Break
5:00 - 6:30	**Session B: Poster Session & Social Hour** Fenn Tower Atrium 5:00 - 5:30 - Welcome from SPS - Fenn Tower 303 5:30 - 6:30 - Poster Session - Fenn Tower 303 / Atrium
6:30 - 8:00	**Banquet** Fenn Tower 303* *Free to Undergraduate Students with SPS Registration. Undergraduate students, please visit the SPS Registration Table to get your free ticket.
8:00 - 8:45	**Session C: After Dinner Speaker** Fenn Tower 303 Communicating Science in the 21st Century: Challenges and Opportunities **Dr. Graham Dixon**, Ohio State University

Saturday October 21

7:45 - 8:15	Registration and Continental Breakfast – SR Atrium
8:15 - 9:00	**HowToREU - An SPS Workshop** SR 152 **Dr. Kiril Streletzky**, SPS President
9:00 - 9:15	Coffee Break
9:15 - 10:00	**Physics Jeopardy** SR 152 Led by CSU SPS
10:00 - 11:00	**SPS Poster session / Lunch Social** SR Atrium & SR 152 Led by CSU SPS
11:00 - 11:45	**Session F: Invited Speaker** SR 151 From Physics to Consulting: Life After the Lab (co-sponsored by EGLS) **Dr. Lisa Felter**, Newry Corp
11:45 - 12:00	**EGLS Chair's Remarks / Student Prizes** SR 151 Dr. Zifeng Yang
12:00 - 1:30	**Physics Department Tour** (Various Labs) Led by CSU SPS

Ohio Section of the American Association of Physics Teachers Meeting
Program Outline

Saturday October 21

7:45 - 8:15	Registration - SR Atrium
8:15 - 9:00	Parallel Pedagogy - Fenn Hall 255 **Dr. Dean Stocker**, UC Blue Ash College
9:00 - 9:15	Coffee Break
9:15 - 10:45	Presentation and Demonstration on Unistellar EVScope - Fenn Hall 255 **Rickey Bartlett, M.Sc.**, Lakeland Community College
10:45 - 11:00	Coffee Break
11:00 - 12:00	**How I do it, Door Prizes and Business Meeting** Fenn Hall 255

ATTENTION UNDERGRADUATES!

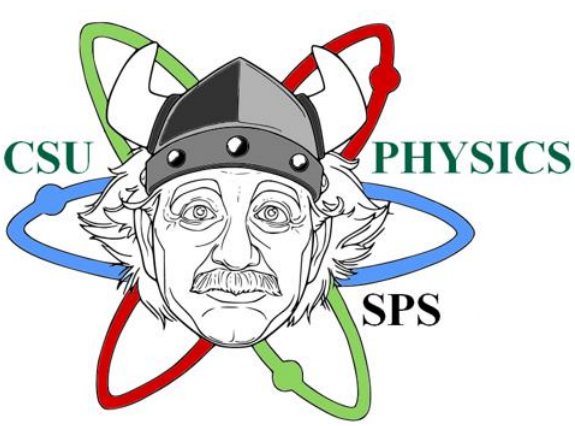

SEE SPS TABLE/FT102 FOR

FREE BANQUET TICKETS